BALTing The Lung Immune Response

Margarida Ferreira Pereira Bobela Kirkby

A dissertation submitted in partial fulfillment of the requirements for the Degree of Masters in Biomedical Research (Specialization Area: OncolBiology) at Faculdade de Ciências Médicas | NOVA Medical School of NOVA University Lisbon

BALTing The Lung Immune Response

Margarida Ferreira Pereira Bobela Kirkby
Supervisors: Luís Graça, Principal Investigator Instituto de Medicina Molecular
Marc Veldhoen, Principal Investigator, Instituto de Medicina Molecular
Duarte Barral, Principal Investigator, Nova Medical School

A dissertation submitted in partial fulfillment of the requirements for the Degree of Masters in Biomedical Research (Specialization Area: Oncology)

September, 2024

The experimental data included in this thesis is sourced from manuscripts in preparation to be published. I hereby state that I have fully participated in the conception, execution and in the validation of the experimental work, in the analysis and interpretation of the collected data as well as in the preparation of the manuscripts.

The experimental work developed in the course of this thesis was approved by the Ethics Research Committee of NMS|FCM-UNL (No. 08/2024/CEFCM).

“There were pages turned with the bridges burned Everything you lose is a step you take”.

“As long as we are fortunate enough to be breathing, we will breathe in, breathe through, breathe deep, breathe out.”

“We are each a patchwork quilt of those who have loved us, those who have believed in our futures, those who showed us empathy and kindness or told us the truth even when it wasn’t easy to hear. Those who told us we could do it when there was absolutely no proof of that.”

- *Taylor Alison Swift*

Funding

The project developd in this master thesis was performed in collaboration between two research groups: Marc Veldhoen Lab “Immune Regulation” and Luís Graça Lab “Lymphocyte Regulation”, under the supervision of Marc Veldhoen, Luís Graça and Duarte Barral, PhD orientation of Jean-Christophe Lone.

This project has received funding from the European Union's Horizon 2020 research and innovation programme under the Marie Skłodowska-Curie grant agreement No: 955321

Outcomes of this thesis:

Poster presentation

Margarida Kirkby, Jean-Christophe Lone, Luis Graça, Marc Veldhoen. BALTing the lung immune response. XLIX Annual Meeting of Portuguese Society for Immunology, Porto (Portugal), 18 April 2024.

Agradecimentos

The past two years, which encompassed the beginning of my master's program and the development of my thesis, have undoubtedly been the most challenging times in my life, marked by countless instances of thinking and saying, “I don’t know how to do this.” I never imagined I would learn so many new techniques and meet so many incredible people who helped me realize that while I most definitely don’t know how to do it, I can learn and grow.

First and foremost, I would like to express my gratitude to my supervisors, Marc Veldhoen and Luís Graça, for welcoming me into their outstanding labs, where I gained invaluable knowledge. Thank you for promoting a good work environment and for helping me always. I also appreciate the opportunity to develop this project alongside my tutor, Jean-Christophe Lone. Lastly, thank you to Professor Duarte Barral, my internal supervisor, who always offered me help when I needed. To JC, thank you for your all your support and for sharing this project with me, even during frustrating times when I messed it up. I am grateful for your patience, your assistance, and for occasionally allowing me to play Taylor Swift during our experimental days, as well as for your generous food and gifts that you stole from events.

I would also like to extend a special thank you to Diana and Vlad, who, despite not having formal tutoring roles, have both taken on mentorship positions. Thank you, Diana, for reviewing my thesis and helping me set timelines, and Vlad, for always answering my many annoying questions (and cries).

To all the lab members from both labs, thank you for your daily support and for being the best coworkers and friends I could have asked for. Marta, Maria, Beatriz, Germano, and Miguel, thank you for making me excited to come to work every day and for filling my lunch hours with so much laughter. You truly made each day at work a joy. I also want to extend my gratitude to the outside members of the lab from IMM, who helped make this place so much brighter.

To my lifelong friends, who may not always understand science and sometimes feel grossed out by my work, thank you for allowing me to share my experiments, presentations, and conferences with you as though you were right there with me. To my closest friends, Carmo, Leo, and Diogo, thank you for your unwavering patience and support throughout this journey, especially during the tough

times in my life. A special thanks to my best friend and favourite designer, Diogo, for your invaluable help with the figures in this thesis.

To Mariana, Renata e Margarida, I am so glad I've meet you three in the beginning of this journey, nothing would've been possible without you. Who else would hear my rantings?

To my family, thank you for your unwavering support, for listening to my mock presentations, and for allowing me to study in the living room while voluntarily refraining from watching TV. To my parents and stepparents, your support throughout this journey has been invaluable, and no words can express my gratitude. Thank you for letting me skip chores when I was overwhelmed with experiments and for always helping me feel more at ease during stressful times.

To my sister, the person who is always by my side, thank you for noticing and loving me even when I'm so stressed I can't speak. Thank you for your conversations and laughs, you are the best sister I could've asked for.

Lastly, I would like to express my heartfelt gratitude to my grandmothers. Avó Bábá, for all the hours teaching me and showing me everything there is to know, you are a force of nature, and I hope to grow into a woman who is a bit like you.

To my Avó são, who came to this country, left her home behind, and worked tirelessly and to this day still inspires me. Thank you, Avó São, for giving me the passion for immunology.

Abstract

Tertiary Lymphoid Structures (TLS) are aggregates of immune cells in non-lymphoid tissue. Located in several organs, they drive immune responses against infections, cancer, and autoimmune diseases. TLS in the lungs, called bronchus-associated lymphoid tissue (BALT) is an ectopic lymphoid structure induced upon infection. In mice, the formation of BALT has been associated with an improved immune response and viral infection control. BALT structurally resembles secondary lymphoid organs (SLO) structures, where the immune response is generated, within a follicle of B cells surrounded by T cells, called the germinal centers (GC). T follicular helper cells (TFH) is one of the main T cell subsets found in BALT. They have the capacity to help B cells generate high-affinity antibodies. The ability to use and manipulate BALT to enhance immune responses presents possibilities for more effective vaccination strategies.

In order to manipulate BALT in the lungs, our aim is to understand how to elicit an effective immune response from this structure. To test this hypothesis, we used three models of infection, the virus *Influenza* X31 (Type 1), the helminth *Nippostrongyllus brasiliensis* (Type 2), and the fungi *Aspergillus fumigatus* (Type 3). Next, we examined BALT formation across various infection types. We hypothesize that BALT formation in the lungs involves the recruitment of TFH cells and that the lung's CD4 helper cell compartment exhibits corresponding polarization to the infection type.

To address this research question, we developed a new infection protocol and used spectral cytometry to study the formation of BALT. After infecting with *Influenza* X31 and *Aspergillus fumigatus*, we observed TFH and GC B cells, which together could be used as a proxy for BALT formation. We visually confirmed these findings with histopathological analysis using H&E staining and immunohistochemistry (IHC). We observed structures in the *Aspergillus*-infected lungs that are presumptive of BALT formation. In the case of Nippostrongylus infection, mainly in the mediastinal lymph nodes, which are known for draining the lung, we also observed an increase in the cell types associated with BALT presence, supporting the idea that TLS can form in the lungs following infection.

Further experiments are necessary to strengthen our findings. In addition, we aim to explore the impact of BALT on the lung microbiome following these three types of infections. These next steps

will help us better understand the role of BALT in lung infections and may provide new insights for treating respiratory diseases.

Resumo

As estruturas linfóides terciárias (TLS[1]) são agregados de células imunitárias em tecido não linfóide. Localizadas em vários órgãos, conduzem a respostas imunitárias contra infeções, tumores e doenças auto-imunes. As TLS nos pulmões - denominadas tecidos linfóides associados aos brônquios (BALT) - são estruturas linfóides ectópicas induzidas por uma infeção. Na experiência efetuada com ratinhos, a formação de BALT foi associada a uma melhor resposta imunitária e ao controlo de infecções virais. O BALT assemelham-se estruturalmente aos órgãos linfóides secundários (SLO), onde é gerada a resposta imunitária, dentro de um folículo de linfócitos B rodeado de linfócitos T. Um dos principais subconjuntos de células T presentes no BALT são as células T foliculares de ajuda (TFH), que desempenham o papel de apoiar na ativação e diferenciação dos linfócitos B a produzir anticorpos de elevada afinidade. A capacidade de utilizar e manipular o BALT, de forma a melhorar as respostas imunitárias, apresenta possibilidades de estratégias de vacinação mais eficazes.

A manipulação do BALT nos pulmões tem como objetivo permitir compreender como se pode obter uma resposta imunitária eficaz a partir daquelas estruturas. Para testar essa hipótese, recorreu-se a três modelos de infeção: o vírus *Influenza X31* (Tipo 1), o parasita *Nippostrongyllus brasiliensis* (Tipo 2) e o fungo *Aspergillus fumigatus* (Tipo 3). Em seguida, foi examinada a formação de BALT em vários tipos de infeção. A hipótese do presente trabalho assenta no facto de que a formação de BALT nos pulmões envolve o recrutamento de células TFH e que o compartimento de células T CD4+ efetoras do pulmão apresenta uma polarização correspondente ao tipo de infeção.

Para responder a esta questão de investigação, foi desenvolvido um novo protocolo de infeção, utilizando a citometria de fluxo espetral, com vista a estudar a formação de BALT. Após a infeção com Influenza X31 e *Aspergillus fumigatus*, observou-se recrutamento de células TFH e de células B do centro germinativo (GC), que, em conjunto, podem ser utilizadas como indicador da formação de BALT. Confirmaram--se visualmente estes resultados com análise histopatológica, utilizando coloração H&E e imunohistoquímica (IHC). Foram observadas estruturas nos pulmões infetados com *Aspergillus,* o que é indicativo da formação de BALT. No caso da infeção por Nippostrongylus, principalmente nos gânglios linfáticos mediastínicos, que são conhecidos por drenar os pulmões, também se observou um aumento dos tipos de células associadas aos BALT, corroborando a ideia de que os TLS podem formar-se nos pulmões após a infeção.

[1] Por uma questão de facilidade de leitura, os acrónimos referenciados correspondem à sua formulação na língua inglesa.

De notar que são necessárias mais experiências para reforçar estes resultados. Adicionalmente iremos estudar o impacto do BALT no microbioma dos pulmões após estas infeções. Nesse sentido, estamos convictos que os próximos passos vão permitir compreender melhor o papel das BALT nas infeções pulmonares e que, nessa perspetiva, podem vir a fornecer novos conhecimentos para o tratamento de doenças.

List of abbreviations

APCs- Antigen-Presenting Cells

TCR- T Cell Receptor

MHC- Major Histocompatibility Complex

SLOs- Secondary Lymphoid Organ

MALT- Mucosal-Associated Lymphoid Tissue

LNs- Lymph Nodes

dLNs- Draining Lymph Nodes

MLNs- Mediastinal Lymph Nodes

SHM: Somatic Hypermutation

GC- Germinal Centers

CSR- Class Switching Recombination

TFH- T Follicular Helper Cell

SAP- Slam Associated Protein

CXCL- Chemokine Ligand

CXCR- Chemokine Receptor

CCR- Chemokine Receptor

HEVs- High Endothelial Venules

IL- Interleukin

LECs- Lymphatic Endothelial Cells

TRM- T Resident Memory Cells

DZ- Dark Zone

LZ- Light Zone

FDCs- Follicular Dendritic Cells

BCR- B Cell Receptor

TLS- Tertiary Lymphoid Structure

BALT- Bronchus-Associated Lymphoid Tissue

DC- Dendritic Cells

FBS- Fetal Bovine Serum

PBS- Phosphate-Buffered Saline

PD-1- Programmed Cell Death Protein

Igs- Immunoglobulins

TCM- T Central Memory Cells

TEM- T Effector Memory Cells

TF- Transcription Factor

Klf2- Krüppel-like Factor 2

Index

1. Introduction

1.1 The immune system overview

1.1.1 Role of T cells in immune responses and Vaccination

Understanding the immune system dynamics within the lungs, is essential for vaccine strategies targeting respiratory infection. Historically, vaccines have significantly reduced the global burden of diseases such as polio, and *Influenza*[1]. However, the continuous evolution of pathogens and the emergence of new infectious threats highlights the urgent need for more sophisticated and adaptable vaccination strategies.

Central to the development of these strategies is a comprehensive understanding of the immune system, particularly the role of T cells in driving and sustaining immune responses, being these cells aim of much research. By focusing on how our body can more effectively activate and engage T cells, it becomes possible to enhance both the efficacy and durability of immune protection, offering broader and longer-lasting defense against disease[2].

Upon encountering a pathogen, the immune system initiates an immune response. T cells, which include various subsets such as helper and cytotoxic T cells, play a central role in clearing infected cells, modulating immune responses, and assisting B cells. B cells are responsible for producing antibodies, proteins that specifically target and neutralize pathogens. T cells also support B cells in generating high-affinity antibodies during germinal center reactions[3]. Together, these processes lead to the formation of memory T and B cells, ensuring rapid and efficient immune responses upon reinfection[4].

The collaboration between T cells and B cells is essential for an effective immune response[5]. By regulating these processes, T cells enhance the overall efficacy of vaccines and contribute significantly to the development of sustained immunological memory, ensuring robust and enduring protection against pathogens[6].

1.1.2 Lymphoid Organs

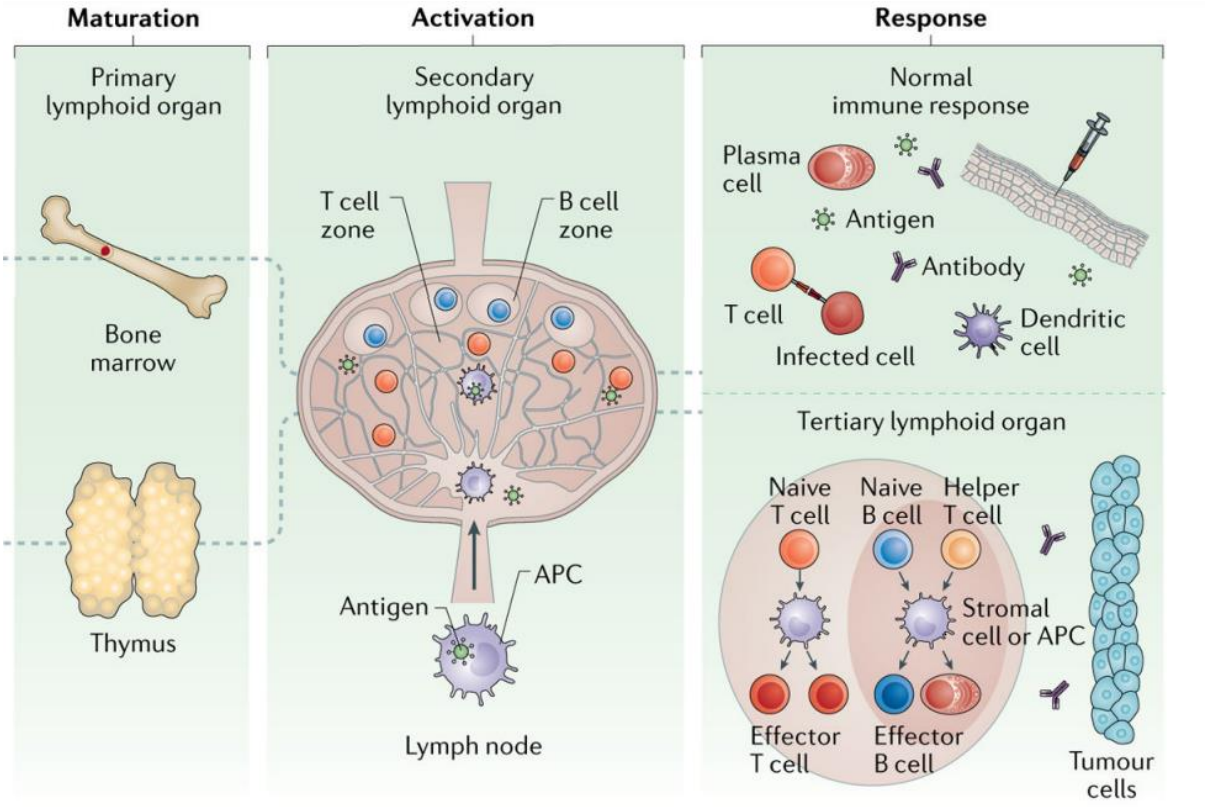

Figure 1- Overview of lymphoid structures and stages of immune response. Primary lymphoid organs are the sites where lymphocytes develop and mature before entering the bloodstream. In SLO, circulating B and T cells are activated upon encountering antigens. Following activation, B cells differentiate into effector cells, such as plasma cells, while T cells differentiate into subsets like cytotoxic T cells**.** Adapted from: Multiscale engineering of immune cells and lymphoid organs [7].

To effectively combat the diverse range of pathogens encountered, the adaptive immune system, composed of T cells and B cells, has evolved to be able to recognize virtually all antigens from bacteria, viruses, and other organisms. B cells use immunoglobulins (Igs) as antigen receptors, producing antibodies upon activation that bind to pathogens in extracellular spaces. CD4 T cells, in contrast, recognize foreign antigens only when presented on the surface of antigen-presenting cells (APCs) via major histocompatibility complex (MHC) molecules to its T cell receptor (TCR). T cells are categorized into CD8+ cytotoxic T cells, which eliminate infected cells, and CD4+ T cells, which activate other immune cells[8]. APCs are also essential for the function of the adaptive immune response, since they are responsible for initiating T cell activation by capturing, processing, and presenting antigens to naïve T cells, which enables the TCR to recognize both self and microbial components[8].

A fundamental aspect of how T cells and B cells operate involves their development and function within lymphoid organs **(Figure *1*).** Lymphoid organs, divided into central (or primary) and peripheral (or secondary) types, have specialized roles in the immune system that distinguish them from non-immune-related organs, such as providing the body with specialized microenvironments for immune activation where lymphocytes can be presented with antigens. Primary lymphoid organs, like the thymus and bone marrow, are the structures where lymphocytes originate and undergo maturation. This is an important process for developing a functional immune system capable of recognizing and responding to a wide variety of pathogens. In contrast, Secondary lymphoid organs (SLOs), such as Lymph nodes (LNs), the spleen, and mucosa-associated lymphoid tissues, are the places where naïve lymphocytes are maintained and where adaptive immune responses are initiated[3,8].

The immune system includes various other lymphoid structures such as Peyer's patches, mucosal-associated lymphoid tissue (MALT), each with distinct features and functions[8,9]. SLOs, form during embryogenesis, independent of antigen recognition, through complex interactions among hematopoietic, mesenchymal, and endothelial cells[9]. They each exhibit distinct features and are dispersed throughout the body. The spleen is an unique structure which is able to sample antigens from the bloodstream. Encapsulated draining LN (dLNs) are key sites where immune cells, such as lymphocytes, interact with antigens and APCs to initiate immune responses. These LNs collect antigens from adjacent non-lymphoid tissues, including mesenteric LN that drain the intestines and mediastinal lymph nodes (mLNs) that drain the upper and lower respiratory tract, particularly from the lungs. In contrast, mucosal lymphoid tissues, directly associated with mucosal surfaces, play an important role in protecting areas such as the gastrointestinal and respiratory tracts[10]. For example, Peyer's patches, located in the lining of the small intestine, have the ability to transport luminal antigens and bacteria, contributing to the immune defense by initiating responses against pathogens entering through the gut[10].

1.1.2.1 Germinal Centers

A defining feature of the adaptive immune system is its capacity to produce antibodies that bind with affinity and specificity to a vast array of antigens[5]. This is facilitated due to structures within SLO, called the germinal centers (GCs). The formation of GCs, in response to infection or immunization, is a key event for the production of T-dependent antibodies[11]. The main

lymphocyte population of these structures is the B cells. The B cells are organized in a follicle, sustained by follicular dendritic cells which role is to maintain this follicular architecture[5] (**Figure 2**). Surrounding this structure, there is an orle of T cells. In GCs, GC B cells undergo a series of changes that differentiate them from their naïve precursors[5]. GC B cells are highly proliferative, they are also larger and more metabolically active than naïve B cells[12]. Within these GCs, several immune processes occur, including somatic hyper mutation, which serves as a basis for B cell affinity maturation (where B cells improve their ability to recognize pathogens), class switch recombination (CSR, which allows B cells to produce different types of antibodies), plasma cell differentiation (B cells becoming antibody-producing cells), and the differentiation of memory B cells, which ensure long-lasting immune protection[5].

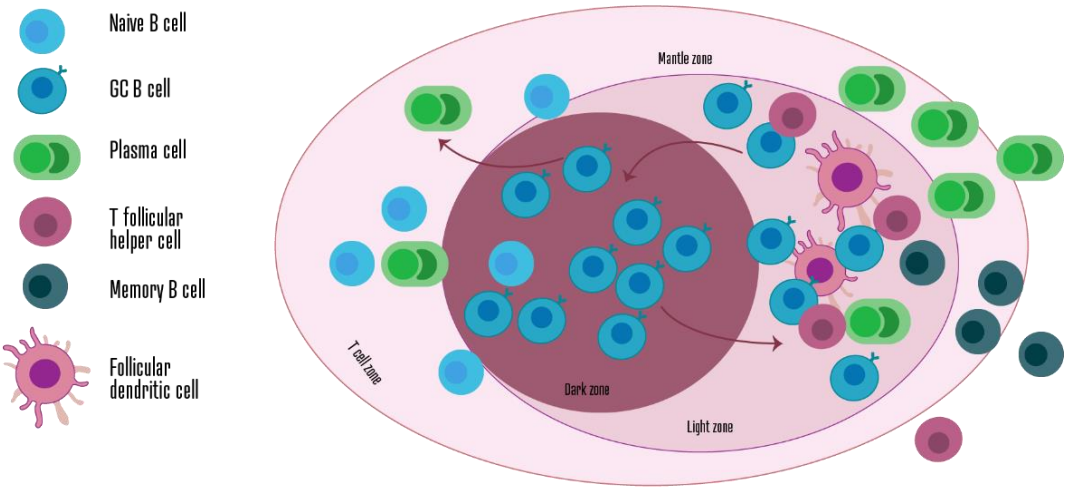

Figure 2- GC reaction overview. The GC is a specialized microenvironment within the B cell follicles of secondary lymphoid tissues, formed in response to infection or immunization. The GC is divided into two main compartments: the dark zone (DZ) and the light zone (LZ). In the DZ, GC B cells undergo proliferation and SHM of their immunoglobulin (Ig) genes. Once GC B cells complete SHM, they enter the LZ. In the LZ, these cells interact with antigens presented by follicular dendritic cells (FDCs) and engage with T follicular helper (TFH) cells for selection. Adapted from: The Germinal Center Milieu in Rheumatoid Arthritis: The Immunological Drummer or Dancer?[13].

GC reaction starts with B cells recognizing specific antigen through their B cell receptor (BCR). Although antigens are mostly presented on the surface of follicular dendritic cells (FDCs), macrophages or dendritic cells, they can also bind directly to soluble antigens[14].

Antigen recognition is followed by the migration of B cells to the border, the T cell zone, facilitated by the upregulation of chemokine receptor CCR7[14], the receptor for T cell zone chemokines CCL21 and CCL19, expressed by naïve CD4+ T cells[15], which facilitates the migration of B cells to this area. At the T-B border, B cells present antigens via MHC Class II molecules to CD4+ helper T cells, which had previously contact with APCs. These T cells provide essential survival and co-stimulatory signals to the B cells[16]. Following this interaction, B cells begin to proliferate at the follicle's perimeter. After this they can either initiate a GC response, forming secondary follicles, or differentiate into memory B cells and plasma cells[11].

After initiating the GC reaction, activated B cells continue to sustain this response with the help of T follicular helper cells (TFH), T cells that help B cells proliferate among other functions. These subset of T cells are able to localize inside the GC[17]. The simultaneous differentiation of both GC B cells and TFH cells is essential for the formation and maintenance of the GC.

1.1.3 Tertiary lymphoid structures

In addition to secondary lymphoid structures, there are lymphoid formations that can develop in non-lymphoid tissues. Known as Tertiary lymphoid structures (TLS) or ectopic lymphoid tissues, these structures are formed postnatally and are composed of immune cells aggregates[18].

They are important in driving antigen-specific immune responses, for instance, TLS are frequently observed in chronic inflammatory conditions, promoting local immune responses and shaping the adaptive immune system's behavior in these sites[19]. They have also been linked to autoimmune diseases[20] and the immune system within tumors, influencing disease

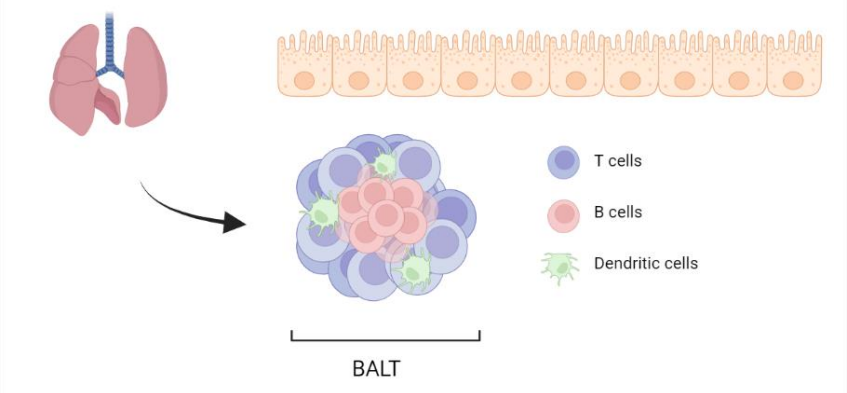

Figure 3- BALT location, structure and composition. BALT is located in the lungs and exhibits a structure similar to a GC, characterized by organized clusters with distinct T and B cell zones. Follicular dendritic cells (FDCs) are present within the structure, situated between these cell areas. Created with Biorender.

outcomes[18]. In the context of respiratory immunity, the lungs provide a unique environment where TLS can form[21]. Typically, lymph from the lungs drains into regional LN, such as mLNs. However, under certain conditions, the lungs can develop TLS directly within their tissue. One prominent example of such a structure is Bronchus-associated lymphoid tissue (BALT), which contributes to local immune responses in the respiratory tract[22].

This structure resembles the GCs present in SLOS **(Figure 3).** In BALT, GC processes mimic what occurs in SLOs, but are adapted to the local environment in the lungs, making BALT a critical part of the respiratory immune response[21]. The T cell population within the TLS can differ, although they are predominantly CD4+ TFH cells[18]. While B and T cell populations constitute the bulk of TLS-associated immune cells, distinct dendritic cell (DC) populations are also present. These DCs, of mesenchymal origin, are vital for the selection of memory B cells during GC reactions[23]. SLOs, together with TLS, form an essential network for immune surveillance and antigen detection, facilitating coordinated immune responses in both lymphoid and non-lymphoid tissues.

1.1.3.1 Follicular Helper Cells and Their Role in TLS

As mentioned before, TLS often contain CD4+ TFH cells and other cell populations such as TFH-like cells. TFH-like cells are a population with phenotypic similarities to T follicular helper (TFH) cells[24]. For example, in the context of cancer, in a mouse model of colitis-associated colon cancer, the formation of tumor-adjacent TLSs was shown to suppress tumor growth. These mice were colonized with *Helicobacter hepaticus* (Hhep), a microbiota species introduced to assess its impact on colorectal cancer (CRC) immunity. This TLS formation was dependent on TFH cells. Experiments done for this paper used $Bcl6^{fl/fl}$ $CD4^{Cre}$, which lack functional TFH cells due to the deletion of Bcl6, a transcription factor essential for TFH cell development. The researchers observed that, without functional TFH cells, the mice were unable to produce an effective anti-tumor response, showing reduced tumor infiltration by immune cells and diminished TLS formation, leading to less tumor control. This phenotype could be rescued by adoptive transfer of TFH cells, which restored TLS formation and tumor suppression, highlighting the role that this population might have in BALT formation, and T cell polarization in the lung[25].

1.1.4 Immune response against infectious agents

The immune system protects the host against invading pathogens and prevents infectious diseases[26], in part, due to adaptive immune responses initiated in lymphoid structures. However, different types of pathogens including viruses, bacteria, fungi, and helminths, can invade the human body. Each of these pathogens utilize distinct strategies to enter and establish infection. Viruses use the host cell's machinery for replication, classifying them as intracellular pathogens. On the other hand, helminths are multicellular organisms that cannot survive within host cells, functioning as extracellular pathogens. Bacteria, fungi, and protozoa occupy an intermediate position, as they can either reside inside or outside host cells, depending on the species. The host's ability to effectively combat an invading pathogen relies heavily on its capacity to generate a suitable protective immune response[26].

Central to the immune response are APCs, naïve lymphocytes, and antigens, as mentioned before. Once activated, T cells proliferate, differentiate, and survive in specialized microenvironments within the lymphoid organs. These environments optimize immune responses by facilitating the development of effector T cells, such as cytotoxic CD8+ T cells, and helper CD4+ T cells[8]. T helper cells are a heterogeneous group that plays an important role in numerous immune responses. While CD4 helper T cells contain several subsets, the primary ones relevant to this work are Th1, Th2, Th17, Tregs, and TFH cells. Dependent on the inflammatory signals, T cells will be polarized towards an appropriate effector phenotype during an infection or immunization[27].

Th1 cells are key mediators in antiviral immunity, primarily through the production of the pro-inflammatory cytokine IFN-γ and are defined by the transcription factor (TF) T-bet. Th2 cells, characterized by the expression of the TF GATA-3, play a critical role in defending the host against helminth infections and toxins. Th17 cells, distinguished by the production of interleukin-17 (IL-27) and regulated by the TF RORγt, are essential for immune responses against extracellular pathogens, particularly within mucosal tissues. These T helper subsets are well characterized for their polarization during specific pathogen encounters[4,24].

Apart from the other T helper cell subsets, there are specialized subsets that have the capacity to support humoral responses[4]. TFH cells have the unique characteristic of accessing the B cell follicle and participate in the GC responses by providing B cell help. TFH cells represent a highly

heterogeneous population, shaped by various factors such as antigenic stimulation, the cytokine milieu within their microenvironment, and other extrinsic signals[17]. Recently it has been described that TFH cells can also specialize themselves according to the type of immune response[27] **(Table 1)**.

Table 1- TFH heterogenity

TFH Subset	Associated Immune Response	Type of Pathogen
Group 1 TFH	Type-1	Intracellular pathogens (e.g., viruses, intracellular bacteria)
Group 2 TFH	Type-2	Extracellular parasites (e.g., helminths)
Group 3 TFH	Type-3	Extracellular bacteria, fungi

The mechanisms underlying TFH cell polarization remain relatively underexplored. However, a deeper understanding of BALT formation and the factors that trigger its development is vital. It is well-established that the structural organization within TLS creates specialized niches that facilitate TFH and B cell interactions, promoting tissue-specific antibody production. Moreover, TFH cells are recognized as the predominant T cell subset within these structures[18]. This knowledge highlights the potential for developing targeted vaccines, highlighting importance of further research into how these T cells can be effectively polarized through vaccination strategies.

Another important T cell compartment is the memory T cells, which play an important role in protecting the body from recurring infections, providing long-term protection[4]. They are functionally and phenotypically classified in at least three subsets. Central memory (TCM) and effector memory (TEM) T cells, which recirculate throughout lymphoid and non-lymphoid organs respectively. Tissue resident memory (TRM) T cells that reside in tissues, especially those at the host/environment interface. TRM cells actively survey the tissues for signs of infection, able to react rapidly and thereby swiftly eliminate infected cells without the need for a systemic immune reaction[28]. TRM cells can be distinguished from circulating

counterparts based on expression of the T cell activation and retention marker CD69 and the αE integrin CD103 for subsets of $CD8^{+}$TRM in mucosal and barrier sites[29]. In CD4 TRM cells, CD103 expression is reduced. However it's still possible to characterize this population using CD69 as a marker[30].

As we know, inflammation and infection in the lung can trigger BALT, it has also been seen that after infection CD4 TRM cells are localized niche structures inside the lung, after re-infection[30]. Possibly the formation of this tissue may allow for TRM cells to stay in the lung and play a role in re-infection.

1.2 Bronchus-associated lymphoid tissue

BALT was first described in 1973 by Bienenstock et al[31,32]. This tertiary lymphoid structure is named after the place where it's predominantly found. BALT is an ectopic lymphoid tissue found in the lungs. Constitutively present in some species, such as rabbits and rats, where it's located along the bifurcations of the upper bronchi[33]. However, BALT is not always found in other species, mice and humans, under physiological conditions. Its formation is induced in different contexts such as chronic inflammation, often associated with autoimmune disease[20] as well, infections[21], and in recent years, the formation of this tissue has also been associated with cancer[18,34].

BALT is not a fixed structure but is shaped by the accumulation and organization of lymphocytes based on local immune needs[33]. Consistent with their immunological functions, infection-associated mucosal ectopic lymphoid structures can produce protective immune responses *in situ*[35]. In this sense, BALT is highly adaptable and can take on different structural characteristics depending on the nature of the immune response[21]. Functionally, BALT serves as a local hub for immune responses within the lungs, enabling the activation of immune cells like T and B cells near the site of infection or inflammation. It plays an important role at sites of infection, facilitating the production of antibodies and the development of immunological memory, that can happen in addition or independently of SLOs[21].

Previous studies on BALT showed that the immune response generated caused less morbidity and mortality when this tissue is developed upon infection, when compared to the immune response only produced from conventional lymphoid organs, also being able to "mimic" the SLOs immune response when these organs are not present[22]. A protective role has also been demonstrated in mouse studies, where BALT was shown to attenuate pulmonary

inflammation[36]. In this case, pre-established BALT can delay the accumulation of lung Th2 cells, usually exacerbated Th2 responses are associated with asthma and other allergic diseases. It also correlates its formation with reduced lung pathology[36].

Another interesting finding about BALT is the fact that it is present in the early life of humans. However its presence declines coincident with the accumulation of memory T cells in the lung[37]. This study supports findings for in situ priming and differentiation of B cells in the lung, showing the presence of GC B cells and TFH. Mainly this study highlights the importance of induction of ectopic lymphoid structures to improve the adaptive immune system when fighting against infections.

Recent studies have shown also the role of TLS and BALT in cancer, presence of TLS in cancer has been correlated with improved prognosis for Non–Small-Cell Lung Cancer[34,38]. In this context, these structures are referred to as tumor-induced BALT (Ti-BALT), and dendritic cells within them have been associated with improved prognosis.

1.2.1 Formation of BALT

Lymphoid organ development requires reciprocal interactions between a variety of lymphoid tissue initiator or inducer cells (LTi) [10]. These cells express common lymphoid chemokines receptors such as CXCR5 and CCR7. They also express lymphotoxin (LT), a cytokine in the TNF superfamily, critical for SLOs formation[39], since through the activation of the Lymphotoxin β receptor on stromal cells it regulates the expression of chemokines like CXCL13, CCL19, and CCL21, which are important for several processes, such as GC reaction[5]. It has been shown that BALT can form independently of LTi cells. However, lymphotoxin remains important for proper organization of BALT. In studies involving mice lacking lymphotoxin, T and B cells fail to segregate effectively, underscoring its role in structuring BALT[10].

Nowadays it is accepted that the first step of inducible BALT development involves the activation and differentiation of stromal cell precursors into BALT-supporting stroma, which includes FDCs, high endothelial venules (HEVs), Thy1+ lymphatic endothelial cells (LECs), and fibroblasts[21] **(Figure 4).** HEVs are specialized blood vessels that enable lymphocytes to migrate from the bloodstream into lymphoid tissues, supporting lymphocyte trafficking into BALT. LECs appear in the lungs after an inflammatory response, particularly surrounding areas of BALT, where they support T cell recruitment and survival by secreting the chemokines, CCL21 and CCL19. Besides HEVs and LECs, the two main types of stromal cells involved in the GC

response, also play a role here[11]. FDCs, which produce CXCL13, and reticular cells (CRCs), which produce CXCL12, work together to help localize B cells. In BALT fibroblasts, specifically CXCL12+ producing fibroblasts, are essential for organizing the B cell follicle structure, attracting B cells via CXCR4, a G-coupled protein receptor, signaling. This process happens similarly to the dark zone of GCs in SLO[21].

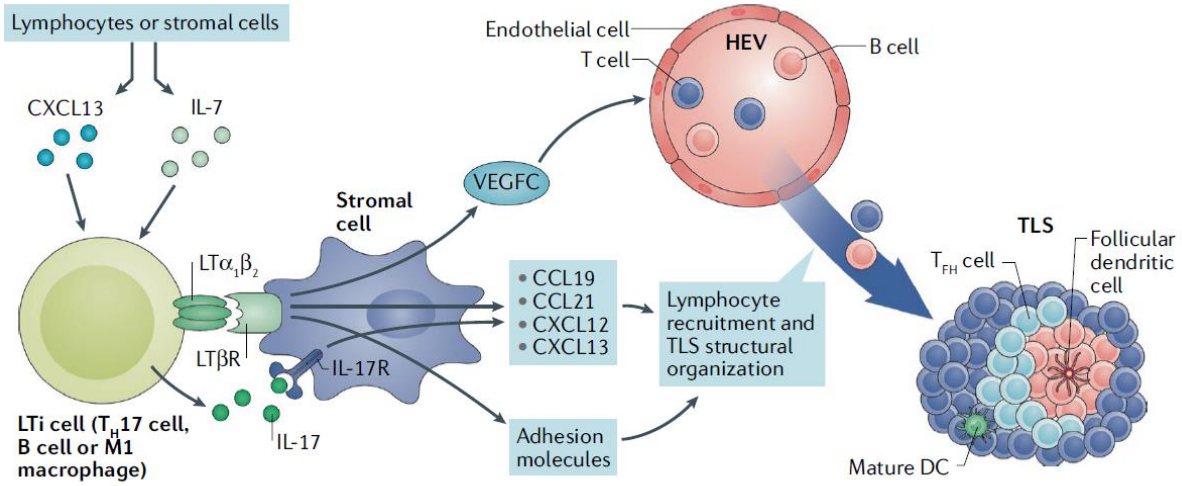

Figure 4- Formation of TLS. Under certain stimuli, antigens may stimulate DCs through the release of various chemokines and cytokines, along with the expression of a unique combination of adhesion molecules on HEVs. This process recruits B and T cells to the site, often organizing them into distinct zones. FDCs reside within the B-cell region, where they present antigens and provide co-stimulatory signals to B cells**.** Retrieved from: "TLS in the era of cancer immunotherapy"[34].

The second stage of BALT development involves leukocyte-mediated inflammation, which promotes the recruitment of B and T cells to the activated stroma, driving the maturation of the BALT structure[21]. As inflammation progresses, the persistent influx of lymphocytes influences the architecture of developing BALT, thereby contributing to its structural organization.

Taken together, these data suggest that the initial phase of inducible BALT development is driven by the differentiation of stromal cells which are capable of recruiting and organizing leukocytes. This process is largely mediated through the production of key chemokines, with CXCL13 and CXCL12 being particularly important in this context, by coordinating the migration and positioning of immune cells[11]. Following this, the accumulation of activated lymphocytes, particularly those expressing lymphotoxin, initiates a positive feedback loop. This loop is

crucial for the stabilization and ongoing maintenance of the BALT structure. The continuous presence of these activated lymphocytes helps to sustain the BALT even after the initial inflammatory stimuli have subsided, ensuring that the tissue remains functional and responsive to future immune challenges[21].

1.2.2 Cellular composition of BALT

Although the composition of this TLS can vary upon their maturation stage, the main lymphocyte population is the B cells. The B cells are organized in a follicle, as stated before, that is sustained by follicular dendritic cells, surrounding this structure there is an orle of T cells.

1.2.2.1 GC B cells

GC B cells are highly proliferative, larger, and more metabolically active than naïve B cells[5]. GC B cells express specific markers that distinguish them from naïve B cells, which can also be used to characterize this population in the lungs[37,40]. One marker is the pro-apoptotic receptor Fas, which is involved in the selection process of GC B cells, ensuring that only those producing high-affinity antibodies survive. Another important marker is n-glycolylneuraminic acid (Neu5Gc), recognized by the antibody GL-7. GL-7 binds specifically to Neu5Gc, which is present on the surface of GC B cells and not on naïve B cells[5]. Central to the regulation of GC B cells is the transcription factor B cell CLL/lymphoma 6 (Bcl6), which is both necessary and sufficient to establish the GC B cell program. The expression of Bcl6 is dependent on B cell activation and is sustained primarily due to the GC reaction, which includes the participation of TFH. This interaction ensures the continued expression of Bcl6 in GC B cells[41]. Since Bcl6 represses *Prdm1*, which encodes Blimp-1, a transcription factor that promotes plasma cell differentiation, by maintaining Bcl6 expression, GC B cells prevent premature differentiation into plasma cells[42].

Regulation of GC responses is characterized by the activated state and rapid proliferation of GC B cells, leading to the formation of two distinct compartments: the dark zone (DZ) and the light zone (LZ)[11].

1.2.2.2 TFH

Discovery of TFH

TFH cells in the context of BALT have not been extensively explored, leaving a significant gap in the understanding of their function in the context of this tissue. Despite this, TFH cells are well-characterized within GCs.

TFH cells are a distinct population of T cells that have received growing interest from researchers since the early 2000s. Prior to this time, TFH cells were poorly described in scientific literature and were often mistaken for other types of T cells, such as CD4+ T helper cells, due to the lack of specific markers and functional understanding of these subset of T cells. However, the T cell role in aiding B cells, was one of the first defined functions of T cells[43]. TFH cells, now recognized as a distinct subset of CD4+ T helper cells, were first characterized by their expression of the surface marker CXCR5, since other CD4 helper cells do not express this marker[44]. CXCR5 is a chemokine receptor expressed by TFH and GC B cells that promotes B and T cell migration toward B cell follicles in response to CXCL13[16]. The importance of CXCR5 in lymphoid tissue organization was established through studies demonstrating its role in the development of LN and Peyer's patches[44]. These studies showed that, in the absence of this receptor, T cells don't migrate inside the follicles. Further research confirmed that CXCL13 (CXCR5 ligand) is essential for B cell migration to follicles, with studies using CXCL13-deficient mice highlighting its function in the development and organization of SLOs[45]. These mice exhibited defects in lymphoid follicle architecture and GC formation, underscoring the role of CXCL13 in guiding B cells into follicles, primarily produced by follicular dendritic cells. Once distinguished from other CD4+ T cells by CXCR5 expression, TFH cells were further characterized by the expression of the TF Bcl6, which serves as the master regulator of TFH cell differentiation. Bcl6 is recognized as a lineage-defining marker of TFH and an antagonist of Blimp-1, which is essential for the differentiation of other T cell subsets[46]. This knowledge separates TFH cells from other T helper cells subsets, each with their distinct TF[24].

The identification of CXCR5 and Bcl6 as defining markers of TFH cells solidified their classification as a unique subset of CD4+ helper cells. However, CD4+ TFH cells are highly heterogeneous, characterized by various distinct markers that can change throughout their lifecycle.

TFH differentiation

Initial Priming of Naïve CD4+ T Cells

TFH cell differentiation is characterized by dynamic cellular migration and interactions with various microenvironments, leading to local diversity among TFH cells[24]. The process of T cell differentiation begins with the priming of naïve CD4+ T cells by DCs, which function as APCs **(Figure 5).** This initial phase involves two essential signals: first, the binding of the TCR on naïve CD4+ T cells to peptide-MHC complexes presented by DCs, and second, co-stimulatory signals provided through the interaction of CD28 on T cells with CD80 or CD86 on DCs[23]. Additionally, the cytokine milieu during this DC-T cell interaction significantly influences the direction of T cell differentiation[16]. This stage marks a critical decision point in T cell fate, as TFH differentiation can be viewed as an early cell fate decision between becoming a TFH cell or differentiating into other non-TFH effector T cell subsets, such as Th1, Th2, or Th17 cells[47].

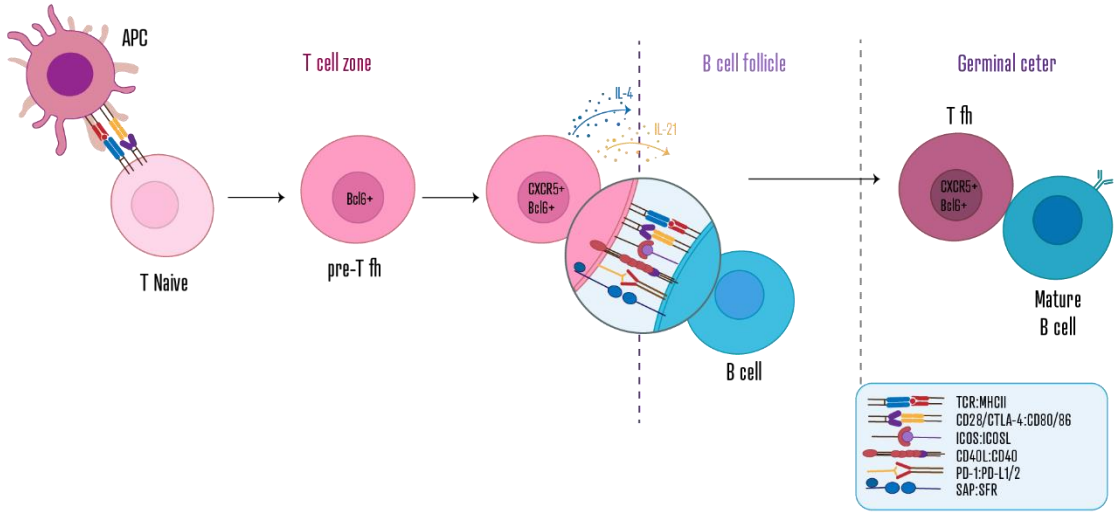

Figure 5- Differentiation of T Follicular Helper TFH Cells within the GC. In the T cell zones of SLO, DCs present peptide antigens via MHC class II molecules to naïve CD4+ T cells. This interaction, recognized by TCR, initiates the activation and clonal expansion of CD4+ T cells. Early during activation, CD4+ T cells begin differentiating into various effector subsets, including TFH cells. A critical step in TFH cell differentiation is the upregulation of the transcription factor Bcl6, which drives the TFH lineage commitment. As TFH cells develop, they express CXCR5, which guides their migration into the B cell zone in response to CXCL13. At the T-B border, CXCR5+ TFH cells interact with antigen-specific B cells. This interaction is facilitated by signals through TCR, CD28-CD80/86 co-stimulatory interactions, and additional signals from ICOS-ICOSL, CD40L-CD40, and PD-1-PD-L1/L2 pathways. These signals collectively enhance TFH function and ensure optimal B cell help. Before they mature into GC (GC) TFH cells, they secrete critical cytokines, such as IL-21 and IL-4, that promote B cell differentiation. Adapted from T follicular Cells: The regulators of GC homeostasis[23].

Expression of Bcl6

A critical decision point in TFH cell differentiation involves the expression of the TF Bcl6. This occurs rapidly during the priming phase of T cell activation and is essential for committing to the TFH cell lineage[23]. Bcl6 functions by suppressing the transcription of genes associated with alternative T helper cell lineages while promoting the expression of TFH cell specific markers. This reciprocal regulation between Bcl-6 and Blimp-1, which drives differentiation into other T helper cell types, is critical for ensuring that T cells commit to the TFH cell fate[46]. This upregulation of Bcl6 occurs at the transcriptional level within hours of antigen exposure[48]. Bcl6 expression induces the upregulation of CXCR5 and repression of CCR7. This allows for the migration of pre-TFH cells into the T-B cell border[23].

Migration of TFH cells

Once TFH cells migrate into the follicles and interact with B cells, they undergo further maturation into GC TFH cells. Importantly, the initial signals from APCs are not sufficient for irreversible TFH cell commitment. For this it is necessary for pre-TFH cell to engage in cognate interactions with antigen-presenting B cells at the T-B border, which are now upregulating CCR7 to move into the periphery of the follicles[49]. This phase of T-B cell interaction occurs in a feedback loop, where both cell subsets cooperate and help each other[23].

T-B cell interactions occur through various mechanisms. The initial T cell-B cell interaction begins before pre-TFH cells are fully developed, aiding B cell proliferation and differentiation through the CD40-CD40L pathway, which is indispensable for the activation of GC B cells. During this phase, pre-TFH cells also produce interleukin-4 (IL-4) and interleukin-21 (IL-21)[17]. Il-4 is known as a B cell survival and differentiation factor, its production is required for optimal B cell activation[50]. IL-21 is known for enhancing B cell proliferation and sustaining the GC program, being highly expressed by TFH cells but not exclusively[17]. It is also recognized as the most potent cytokine for driving plasma cell differentiation in both mice and humans[51].

Nevertheless, stable T-B cell junctions form through mechanisms such as peptide-MHCII and ICOS-ICOSL binding. ICOS co-stimulation is particularly important for TFH cells as it maintains their phenotype, location and production of cytokines essential for B cell survival[17,23]. ICOS/ICOSL signaling helps maintain low levels of Krüppel-like factor 2 (Klf2), which regulates the expression of homing genes like *CCR7* and *CXCR5,* maintaining CXCR5 expression and low

level of CCR7. Studies have shown that ICOS blockade leads to the localization of TFH cells in T cell zones, highlighting its role[23].

SLAM-associated protein (SAP) and programmed cell death protein (PD-1) expression gradually increase as TFH gain a more mature phenotype[23]. As TFH travel inside the GC and the T-B cells junction need to be maintained, which is done by integrins and SAP[17,24]. These stable interactions are necessary for the subsequent proliferation of both TFH and B cells and their commitment to the GC fate[52]. Additionally, PD-1 plays a significant role in GC TFH cells by inhibition of TCR signaling and CD28 co-stimulation, as well as CXCR3 upregulation, that further promotes retention within the GC[53]. PD-L1, expressed by bystander B cells in the follicular mantle, further prevents the loss of TFH cells from the GC, highlighting the importance of PD-1 in sustaining the GC reaction[17].

GC TFH cells exhibit high motility, enabling dynamic interactions with GC B cells that are critical for selecting high-affinity B cells and promoting effective antibody responses, as well as the formation of TLS. As described, throughout their differentiation, TFH cells are characterized by a complex interplay of transcriptional regulators, signaling pathways, and cell-cell interactions, ensuring TFH cells can effectively support B cell maturation, affinity maturation, and the generation of robust, long-lasting humoral immunity.

Considering the important role of TFH cells in mediating interactions with B cells within germinal centers, it is imperative to further investigate their functions within bronchus-associated lymphoid tissue (BALT). This study emphasizes the significance of ectopic lymphoid structures in enhancing the adaptive immune response, particularly regarding respiratory infections.

2. Methods and materials

2.1 Mice

C57BL/6J (wild type) mice were obtained from either from the rodent facility at the Instituto de Medicina Molecular João Lobo Antunes (iMM) or from Charles River Laboratories. All mice were housed in a specific pathogen-free (SPF) environment within the IMM (instituto de medicina molecular) rodent facility, compliant with biosafety level 2 (BSL2) standards, which allows for the use of infectious agents. The mice were kept on a 12-hour light/dark cycle with controlled temperature and humidity, and they had ad libitum access to standard chow and water. All the mice were between 7-9 weeks old and animals were sex matched in each experiment. All experiments were approved by Direção Geral de Alimentação e Veterinária (DGAV) in accordance with national and EU regulations. The number of mice used per experiment is described in supplementary data. **(Table S1)**

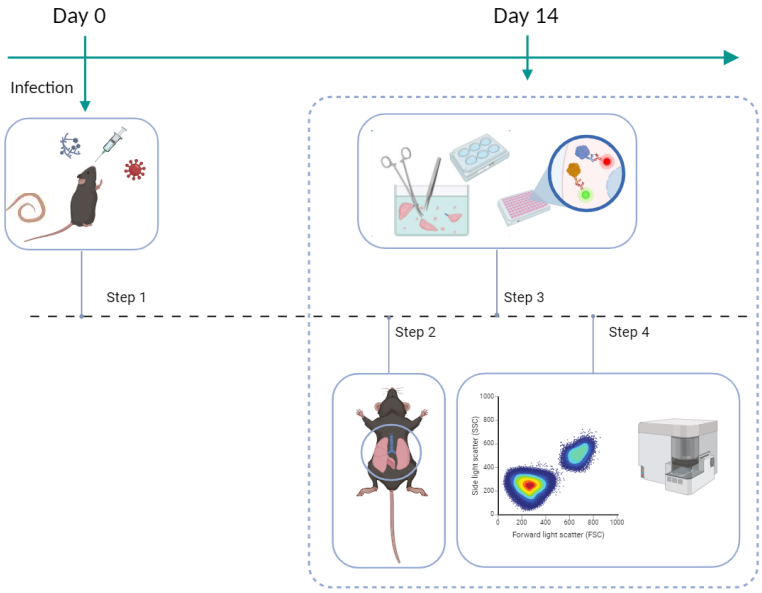

Figure 6- Experimental workflow. Mice are infected on day 0 and weighed daily until day 13. After this period, the mice are dissected, and their organs (lymph nodes, lungs, and spleen) are processed individually into single-cell suspensions. These suspensions are analyzed using spectral flow cytometry to assess immune cell populations.

2.2 Infections

Infections were performed under sterile conditions inside a laminar flow hood, ensuring a controlled and pathogen-free environment. All procedures were conducted in specific pathogen-free (SPF) conditions to prevent contamination. It is typical for animals to experience weight loss following infection. To monitor the overall health and progression of

the infection, mouse body weight was measured daily for 14 days post-infection **(Figure 6)**. Control groups were infected with Phosphate-buffered saline (PBS (0.1 M, pH 7.4)) to determine whether the observed weight loss resulted from the infection or the stress of the procedure

Three different infections were administered:

Influenza A/X-31 **Infection:** Mice were intranasally infected with 1500, 3000, or 5000 plaque-forming units (PFU) of *Influenza* A virus (strain A/X-31 H3N2). This strain is a genetically modified variant that combines elements from two different *Influenza* strains, utilizing Hemagglutinin subtype 3 (HA) and Neuraminidase subtype 2 (NA) to enhance its infectivity and study host responses. The total volume of the viral inoculum was 30 µL, diluted in PBS. This viral strain was generously provided by Marta Alenquer from the Maria João Amorim lab at the Instituto Gulbenkian de Ciência. The virus stock was stored at -80°C and thawed at room temperature immediately prior to use to ensure optimal viability and effectiveness for the infections.

Aspergillus fumigatus **infection:** Mice were intranasally inoculated with 10^8 *Aspergillus fumigatus* conidia in 30 µL of solution, administered twice with a 48-hour interval between doses. The conidia were provided by Patricia Gonçalves from the Cristina Silva Pereira lab at the Instituto de Tecnologia Química e Biológica (ITQB). The conidia, which had been previously stored at -80°C, were defrosted in stages, first at -20°C and then at 4°C, before being cultured on Sabouraud Dextrose Agar (SDA) at 37°C for two days. Fresh conidia were collected from ITQB for immediate use for infection.

Nippostrongylus brasiliensis **infection** Mice were subcutaneously infected with 500 *N. brasiliensis* worms, suspended in 100 µL of PBS. The worms were supplied by Brian Chan from Judith Allen's lab at the University of Manchester. After shipment to our lab, they were prepared on the day of infection using a modified Baermann's technique. For this preparation, a 50 mL Falcon tube was filled with 45 mL of pre-warmed PBS (37°C) and covered with gauze. The worms, housed on wet filter paper in petri dishes, were placed on top of the gauze, ensuring the bottom of the gauze was submerged in PBS. The setup was incubated at 37°C for at least two hours, allowing the worms to actively migrate through the gauze and settle at the

conical base of the tube. The worms were then collected using a micropipette and counted under a microscope to achieve a concentration of 500 larvae per 100 µL of PBS.

2.3 Organ Collection and Processing

At the chosen time points, mice were euthanized by cervical dislocation. Spleens, lungs, and mLNs were immediately collected and placed in ice-cold PBS for processing. Single-cell suspensions were prepared from each organ.

For the spleens and LNs, tissues were mechanically disrupted by meshing through a 50 µm cell strainer. Washed with PBS The samples were centrifuged at 500xg for 5 minutes. After this step, the lymph node pellet is ready to be resuspended and plated in 96-U-bottom wells. The spleen cell pellets were resuspended in 1 mL of ACK lysis buffer (150 mM NH_4Cl, 10 mM $KHCO_3$, 0.1 mM Na_2EDTA) to lyse red blood cells, incubated for 3 minutes, then washed and resuspended in PBS, ready to be plated.

For lung processing, both mechanical and enzymatic digestion are required. Lung's structure includes collagen and elastin, making it more resistant to mechanical dissociation. This mixture consists of Liberase TL (Roche, 05401020001) concentration of 0.1 mg/mL, with the purpose of tissue dissociation and DNase I (Roche, 10104159001) at 1 mg/mL, which degrades DNA from dead cells. The lung samples are incubated in this enzymatic solution at 37°C with shaking at 100 RPM for 30 minutes. To stop the digestion, ice-cold PBS with 5% fetal bovine serum (FBS) is added. The tissue is then passed through a 50 µm cell strainer for additional mechanical disruption. Finally, after an ACK lysis step, as performed for the spleen samples, cells are washed, and the resulting pellets are resuspended in PBS for subsequent analysis.

2.4 Cellular Preparation, Staining, and Flow Cytometry Analysis

Cell suspensions from the spleen, lungs, and LNs were transferred to U-bottom 96-well plates for analysis. To assess surface markers, cells were stained using the antibody panel listed in **Table S2**. Surface staining was conducted in FACS buffer at 4°C for 2 hours, utilizing 100 µL of the master mix (MM) to ensure sufficient volume for accurate pipetting of antibodies. The master mix is a pre-prepared solution that contains all necessary antibodies in the correct dilutions, allowing for consistent and efficient staining. Following surface staining, the cells

were fixed using eBioscience™ IC Fixation Buffer (ThermoFisher, 00-8222-49) at room temperature for 40 minutes. After fixation, the cells were washed and resuspended in PBS until flow cytometry analysis.

For intracellular marker analysis, cells were first fixed and permeabilized using the eBioscience™ Foxp3 / Transcription Factor Staining Buffer Set (Invitrogen) after the initial surface staining. Following a 40-minute fixation at 4°C, the samples were washed with permeabilization buffer. Cells were then stained with the master mix (MM), applying 100 µL per well. This staining process was performed for 30 minutes, using the antibodies in **Table S3**. Finally, the cells were resuspended in PBS and prepared for flow cytometry analysis.

The stained single-cell suspensions were analyzed using spectral flow cytometry on the Cytek Aurora (Cytek Biosciences). Data acquisition using SpectroFlo® software and analysis using FlowJo v9 software (TreeStar).

2.5 Histology

Lungs were collected, fixed in formalin, embedded in paraffin, and sectioned. Hematoxylin and eosin (H&E) staining was performed to assess tissue morphology. For immunohistochemistry, sections were stained with anti-CD20 to identify B cells and anti-CD3 for B cells, **Table S4.** Samples were sent to Instituto Gulbenkian de Ciência (IGC) for pathology assessment.

2.6 Statistical Analysis

Statistical analyses were performed using GraphPad Prism 9 (GraphPad Software Inc.). Data were analyzed using tests specified in the figure legends. Data are expressed as mean ± standard deviation; *p<0.05, **p<0.01, ***p<0.001, ****p<0.0001. Each dot represents a mouse.

3. Hypothesis and objectives

Bronchus-associated lymphoid tissue (BALT) plays an important role in the immune response in the lungs. However, it remains understudied. Despite its relevance in mucosal immunity, BALT has often been overlooked due to its delayed formation and immune response compared to other lymphoid structures. This has resulted in limited knowledge about the stimuli that trigger its formation, the specific immune cell populations involved, and how T helper cells are polarized within this structure. Understanding these aspects is necessary to fully explore the role of BALT in immune responses during respiratory infections and to potentially use it in the development of better vaccination strategies.

We hypothesize that BALT formation is driven by pathogen-specific stimuli, involving the recruitment of TFH cells, which facilitate B cell responses, and the polarization of CD4+ T helper cells in an infection-dependent way.

The objective of this study is to investigate the formation of BALT across different infection models: *Influenza X31, Nippostrongylus brasiliensis*, and *Aspergillus fumigatus*. To characterize the cellular composition of BALT, with a particular focus on TFH cell recruitment and T helper cell polarization. Through the application of advanced techniques, including spectral cytometry and histopathological analysis, we seek to understand what triggers the formation of BALT in the lung. This understanding will bring us closer to developing strategies to modulate BALT and enhance immune responses, particularly in optimizing vaccination approaches.

4. Results

4.1 Surface Staining Shows CXCR5 cleavage in the Lungs During Digestion

The objective of this experiment was to establish if BALT forms after *Influenza* infection by determining the presence of TFH cells. We hypothesized that TFH cells would be present in the lungs if BALT forms, as these cells are essential for supporting B cell responses in lymphoid structures. If BALT does not form, we would expect little to no increase in TFH cells, as they typically reside in SLOs.

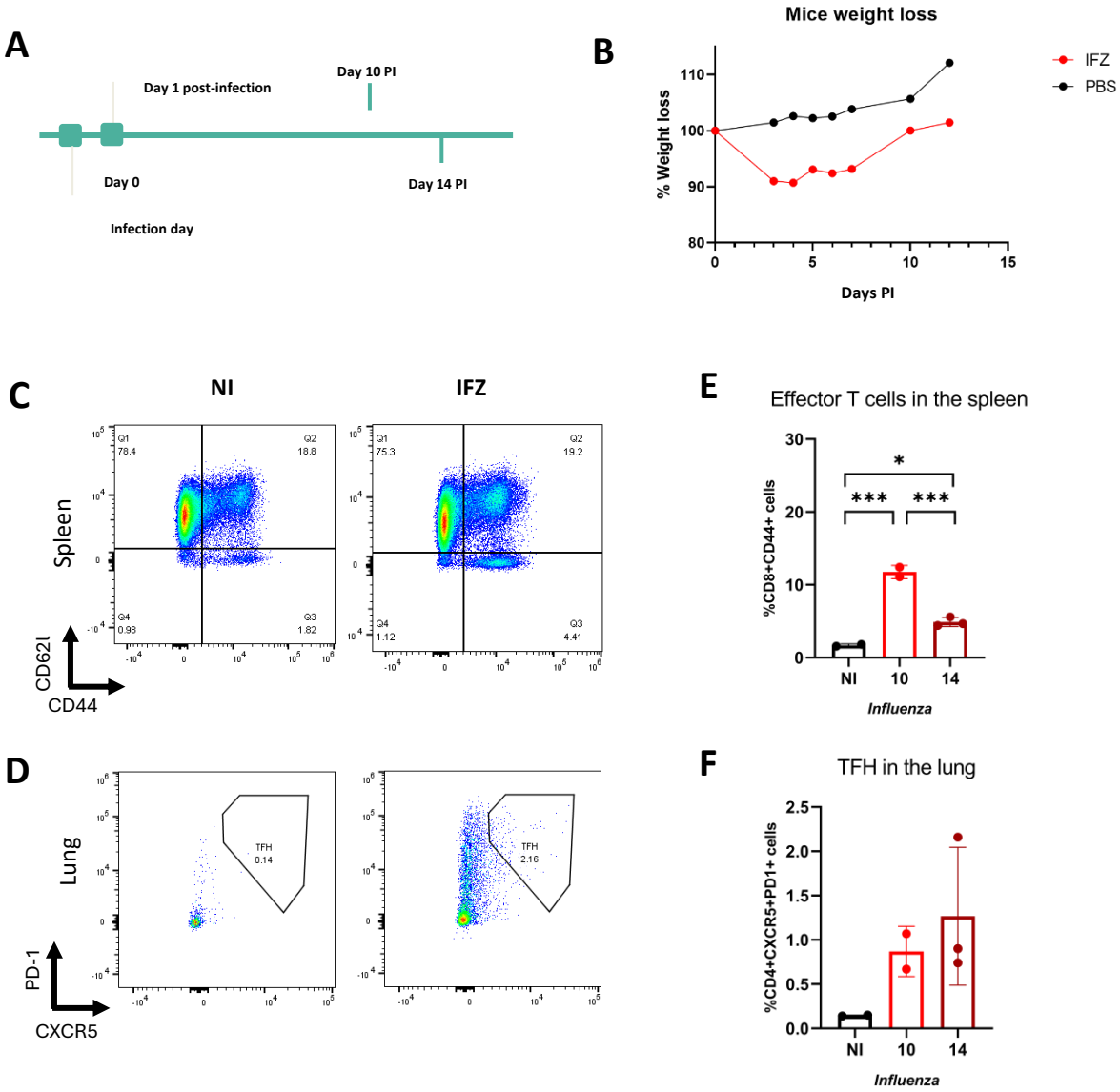

Figure 7- Surface Staining Shows CXCR5 cleavage in the Lungs During Digestion (A) Experimental timeline for *Influenza* infection with 1500 PFU, with two time points: 10 and 14 days post-infection. **(B)** Mice weight loss post-infection, comparing infected and non-infected animals. **(C-D)** Representative dot plots: **(C)** recruitment of Effector CD8+ T cells (CD44+) 14 days upon infection in the spleen. **(D)** TFH cells marked by (CXCR5+ PD-1+) in the lungs 14 days post-infection. **(E-F)** Bar plots: **(E)** Frequency of effector T cells in the spleen. **(F)** Frequency of TFH cells in the lungs. Data are expressed as mean ± standard deviation. Statistical significance was assessed using one-way ANOVA with Tukey's multiple comparisons test. Each dot represents a mouse.

This experiment was performed on two different time point after infection, on day 10 and 14 where we hypothesized there will be BALT formation **(Figure 7A**). *Influenza* Infection was confirmed by monitoring weight loss in infected mice, which is a typical symptom of acute *Influenza* infection. Weight loss began around day 4 and showed signs of recovery by day 7 or 8 **(Figure 7B).** A significant reduction in weight was observed in infected mice compared to non-infected controls, these clinical symptoms are used to confirm the infection worked. To confirm success of infection, we evaluated the immune response by assessing the population of effector CD8+ T cells (CD44+ CD62L-) in the lungs and spleen at 10 and 14 days post-infection. Effector T cells were identified using CD62L and CD44 markers. Gating strategy for flow cytometry experiments is represented in supplementary data **(Figure S 1).** CD62Llow indicates naïve T cells, while CD44high marks cells that have been activated by antigen exposure. As expected, we observed an increased percentage of effector CD8+ T cells in both the lungs and spleen at these time points **(Figure 7 C, E),** demonstrating effective T cell activation and recruitment, due to infection.

To examine the TFH cell population (CXCR5+ PD-1+) in the lungs, we hypothesized that if BALT formation occurs post-*Influenza* infection, TFH cells would be detectable. TFH cells are typically identified using two classical markers in flow cytometry: CXCR5, a chemokine receptor from the GPCR family, and PD-1, which regulates selection and survival in GCs. However, flow cytometry analysis revealed no significant increase in either the number or frequency of TFH cells in the lungs of infected mice compared to non-infected controls **(Figure 7D, F)**. In contrast, a clear presence of TFH cells was detected in the spleen post-infection, indicating that these cells are prominent in SLOs during *Influenza* infection. Subsequently, we considered the possibility that TFH cells might be present in the lungs, but their CXCR5 expression was not detectable via flow cytometry. A review of the literature revealed that enzymatic digestion protocols used to process lung tissue may cleave CXCR5 receptor, preventing its detection. Our own use of a 15-minute surface staining protocol failed to detect CXCR5. These findings highlight the need for troubleshooting of this protocol to confirm the presence of TFH cells in the lungs.

4.2 Optimal *Influenza* Viral Load for Inducing BALT Formation

The objective of this experiment was to determine whether higher *Influenza* X31 viral loads are necessary to induce BALT formation, which we hypothesized might be reflected by an increase in key immune cell populations: TFH, TRM, and GC B cells. If our hypothesis is correct, we would expect to observe an increase in these populations with higher viral loads.

To test this, we infected mice with different doses of the virus (1500, 3000, and 5000 PFU) and monitored weight loss as an indicator of infection severity, in line with ethical guidelines that limit weight loss to under 20%. As shown **(Figure 8B),** weight loss increased with viral dose, in a

dose-dependent manner, with the highest dose (5000 PFU) resulting in the greatest weight loss, though still within acceptable limits.

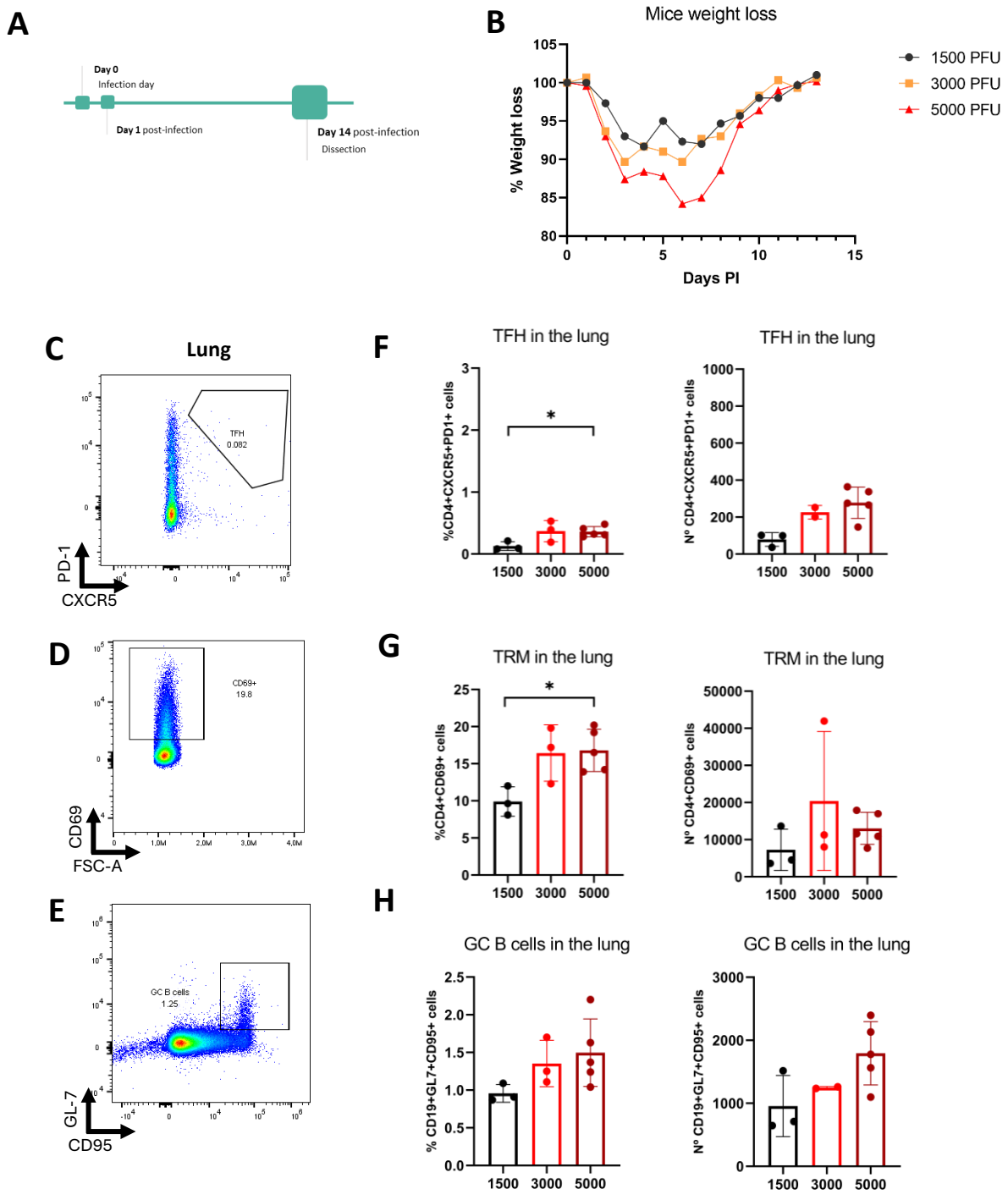

Figure 8- Optimal *Influenza* Viral Load for Inducing BALT Formation (A) Experimental timeline with a single time point at 14 days post-infection. **(B)** Mice weight loss between groups with different doses of viral load. **(C-E)** Representative flow cytometry dot plots of *Influenza* infected mice: **(C)** TFH cells (CXCR5+ PD-1+) in the lung. **(D)** TRM population (CD69+ CD4+) in the lung. **(E)** GC B cells (GL-7+ CD95+) in the lung. **(F-H)** Bar plots: **(F)** Frequency (left) and absolute numbers (right) of TFH cells in the lung. **(G)** Frequency (left) and absolute numbers (right) of TRM cells in the lung. **(H)** Frequency (left) and absolute numbers (right) of GC B cells in the lung. Data are expressed as mean ± standard deviation; Statistical significance was assessed using one-way ANOVA with Tukey's multiple comparisons test. Each dot represents a mouse.

Following infection, we confirmed immune activation by analyzing the recruitment of effector cells (CD44+ within CD8+ T cells) in both the spleen and lung using flow cytometry **(Figure S 3, A-C).** While recruitment occurred across all viral doses, the differences between them were not statistically significant.

In addition to monitoring effector cells, we assessed the impact of viral load on the TFH cell population (CXCR5+ PD-1+) in the lung **(Figure 8 C, F)**. A slight increase in TFH cells was observed with the highest viral dose 5000 PFU, when compared to the 1500 PFU group. Based on this, we focused on the 5000 PFU dose, hypothesizing that a higher TFH presence correlates with increased immune activity and BALT formation.

We also evaluated the TRM and GC B cell populations. TRM cells, identified by CD69+ expression within CD4+ T cells (**Figure 8 D, G)**, were present in the lung at 14 days post-infection, although no significant variation was observed between viral doses. CD69 has a role in retaining TRM cells in the tissue, allowing us to assess TRM immune responses. GC B cells, marked by GL-7 and CD95 **(Figure 8E, H)**, were analyzed for their role in GC formation and selection. CD95, also known as Fas, is a pro-apoptotic receptor involved in the selection process within GCs, ensuring that only B cells producing high-affinity antibodies survive. GL-7 binds specifically to n-glycolylneuraminic acid (Neu5Gc), a marker present on GC B cells but absent on naïve B cells. While GC B cells were detected, no significant differences were observed across the viral doses.

In conclusion, the data suggest that the 5000 PFU viral load offers the greatest potential for inducing BALT formation, as reflected by the increased presence of TFH cells and stable TRM and GC B cell populations in the lungs.

4.3 BALT Formation and Immune Cell Dynamics at Different Time Points Following Influenza Infection

The objective of this experiment was to investigate whether BALT is maintained over time following *Influenza* infection, and whether the associated immune cell populations, TFH, GC B, and TRM cells change dynamically in the lungs and mLNs at different time points post-infection. If BALT formation is sustained throughout the infection, we would expect to observe TFH cell presence in both the lungs and mLNs over time, along with detectable GC B cells and TRM cells at all time points.

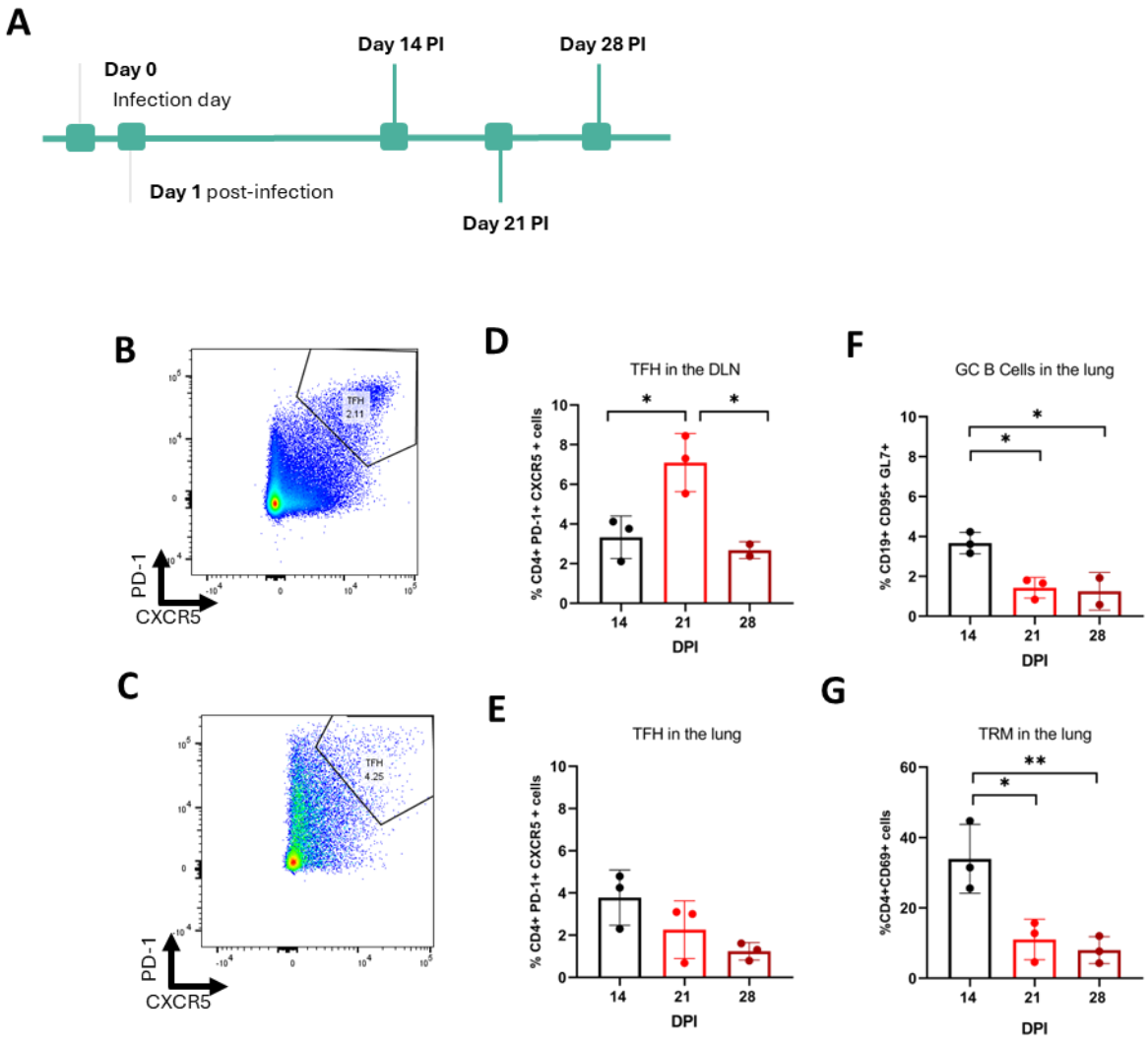

Figure 9- BALT Formation and Immune Cell Dynamics at Different Time Points Following *Influenza* Infection
(A) Experimental timeline showing time points at 14, 21, and 28 days post-infection. **(B,C)** Representative dot plots: **(B)** TFH CD4+ T cells in the dLNs and **(C)** lungs of infected and non-infected (NI) animals. **(D-G)** Bar plots: **(D)** Frequency of TFH cells in the dLNs across different time points. **(E)** Frequency of TFH cells in the lungs at 14, 21, and 28 days post-infection. **(F)** Frequency of GC B cells in the lungs at different time-points. **(G)** Frequency of TRM cells in the lungs post-infection, over different time-points. Each dot represents a mouse.

To test this, we analyzed three distinct time points 14, 21, and 28 days post-infection **(Figure 9A)**, and included the mLNs, as they drain the lungs and may contain immune cells, serving as a proxy for analyze of lung immune cells. As in earlier experiments, infection severity was confirmed by tracking weight loss **(Figure S 4A),** and effector cell recruitment in the spleen was verified by flow cytometry, which showed consistent responses **(Figure S 4B).**

A key aspect of this experiment was optimizing TFH cell detection through changes in tissue digestion protocols and staining time. Given that enzymatic digestion has been shown to affect CXCR5 expression, potentially leading to under-detection of CXCR5+ TFH cells, we

applied both mechanical and enzymatic digestion to the spleen to assess the impact of enzymatic digestion on CXCR5 expression **(Figure S 4C).** We also tested surface staining times, ranging from 15 minutes to 4 hours, and found that a 2-hour staining period provided optimal TFH cells detection without compromising cell viability for both lungs and spleen **(Figure S 4D).** Using this optimized staining protocol, we detected significantly more CXCR5 expression which means it was possible to observe more TFH cells in the lungs than in earlier experiments **(Figure 9C)**.

The data from this experiment **(Figure 9, B)** shows that TFH cells were present in the mLNs, with the highest frequency **(Figure 9D)** and absolute numbers **(Figure S 4G)** detected at 21 days post-infection. In the lungs, TFH cell numbers **(Figure S 4E)** were notably higher than in previous experiments, but there were no significant changes between 14, 21, and 28 days **(Figure 9 E).**

For GC B cells **(Figure 9F),** the highest frequency was observed at day 14, when compared to the other two time points, but no significant differences were found in absolute numbers across time points **(Figure S 4F).** Similarly, the TRM cell population **(Figure 9G)** showed higher frequencies at day 14, though the differences in absolute numbers were not significant **(Figure S 4H).**

In conclusion, this experiment demonstrates that TFH cells, GC B cells, and TRM cells are present at multiple time points post-infection, supporting the hypothesis that BALT may be sustained throughout the infection course.

4.4 BALT is formed upon three different infection types

This experiment investigated BALT formation across different infections *Aspergillus*, *Nippostrongylus*, and *Influenza* at three time points: 7, 14, and 21 days post-infection **(Figure *10*A)**. Lung analyses were only conducted at day 14, as other lung samples were reserved for microbiome sequencing, which we will not discuss in this work. Infection readout was monitored by weight loss, with clear distinctions between control and infected groups **(Figure 10B).** To observe the recruitment of effector cells, as a measure of infection success, spleen cell population from all infections were also analyzed (Data not shown). To understand if BALT was formed after all infection types, we assessed TFH, TRM and GC B cells populations in the mLNs and lungs.

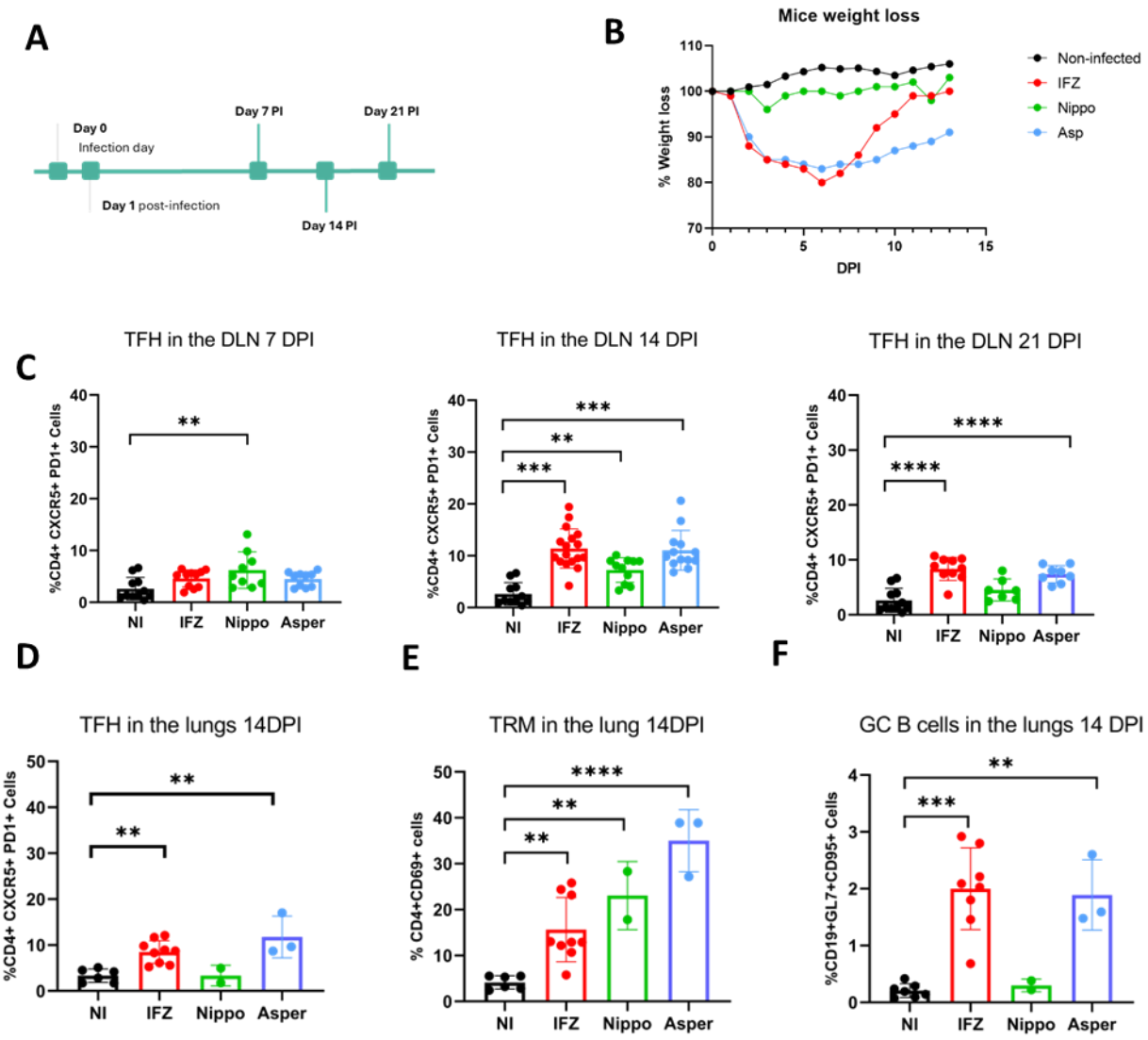

Figure 10- BALT is formed upon three different infection types. (A) Experimental timeline showing three time points at 7, 14, and 21 days post-infection. **(B)** Mice weight loss was used as a clinical readout for infection efficacy. **(C-F)** Histogram plots comparing all infections: **(C)** TFH cell presence in the mLNs as frequency across three time points: 7 DPI (left), 14 DPI (middle), and 21 DPI (right). **(D)** TFH cell frequency in the lungs across all infections at 14 days post-infection. **(E)** GC B cells as frequency in the lungs across all infections at 14 days post-infection. **(F)** TRM cell frequency in the lungs across all infections at 14 days post-infection. Statistical analysis was performed using one-way ANOVA followed by Tukey's multiple comparisons test. Each dot represents a mouse.

At day 7, TFH cells in the DLN were significantly elevated in *Nippostrongylus*-infected mice compared to controls, while *Aspergillus* and *Influenza* infections showed lower TFH frequencies comparing to other time-points **(Figure 10C).** By day 14, TFH cell frequencies **(Figure 10 C, left)** and absolute numbers **(*Figure S 5*A)** were significantly higher in the DLNs of *Aspergillus* and *Influenza* infected mice compared to controls and *Nippostrongylus,* although not as much **(Figure 10C).** This trend continued at day 21, with both *Aspergillus* and *Influenza* infections showing the highest TFH presence in frequency when comparing with the non-infected group **(Figure 10C, right).**

At day 14, TFH cells in the lungs of *Influenza*-infected mice were more detectable compared to previous experiments. The switch from collagenase A to Liberase TL in the tissue digestion protocol, combined with a 2-hour surface staining, significantly enhanced TFH cell detection. Results showed a notable recruiment of TFH cell populations across *Influenza* and *Aspergillus* infections **(Figure 10D-E),** showing higher TFH cell percentages when compared to *Nippostrongylus* and controls. *Aspergillus* infection, in particular, demonstrated the most pronounced presence of total TFH cell numbers **(Figure S 5C).** After *Influenza* and *Aspergillus* infections, the percentage of GC B cells increased **(Figure 10F)**, compared to control groups, with the absolute number of GC B cells being significantly higher in *Aspergillus*-infected mice **(Figure S 5D).** TRM cell population was also analyzed **(Figure 10F)**. Both frequency **(Figure 10E)** and total numbers **(Figure S 5E)** were highest in *Aspergillus* infection, although the TRM frequency was elevated in *Influenza* and *Nippostrongylus* infections compared to controls **(Figure 10E).**

In summary, these results serve as a proxy to confirm that BALT formation occurred following *Aspergillus* and *Influenza* infections, with dynamic changes in TFH, TRM, and GC B cell populations over time. BALT development and immune cell populations were most prominent following *Aspergillus* infection, particularly at earlier time points, indicating that infection type and duration significantly influence BALT dynamics.

4.5 T helper cell polarization changes according to infection type

The objective of this experiment was to determine T helper cell polarization in the lungs 14 days post-infection using spectral flow cytometry **(Figure 11).** By analyzing key intracellular markers: Bcl6 for TFH cells, Foxp3 for Tregs, GATA3 for Th2 cells, RORγt for Th17 cells, and T-bet for Th1 cells. We aimed to identify the specific T helper cell populations activated in response to each type of infection. We hypothesized that each infection would drive distinct polarization patterns, reflected by the upregulation of corresponding TF in CD4+ T cells. We started by analyzing *Influenza* infection **(Figure 11B).** Our hypothesis was that *Influenza* would primarily induce a type 1 immune response, characterized by increased T-bet expression. The results confirmed this, as we observed a significant upregulation of T-bet, both in terms of frequency **(Figure 11B, left)** and total cell numbers **(Figure 11B, right).** This shows that CD4+ T cells were polarized toward a Th1 cell response. In addition to T-bet, we saw a marked increase in Foxp3 expression, indicating that Tregs were also recruited in response to *Influenza* infection.

These findings are in line with the hypothesis that *Influenza* promotes a Th1 cell-dominant response while also engaging Treg populations.

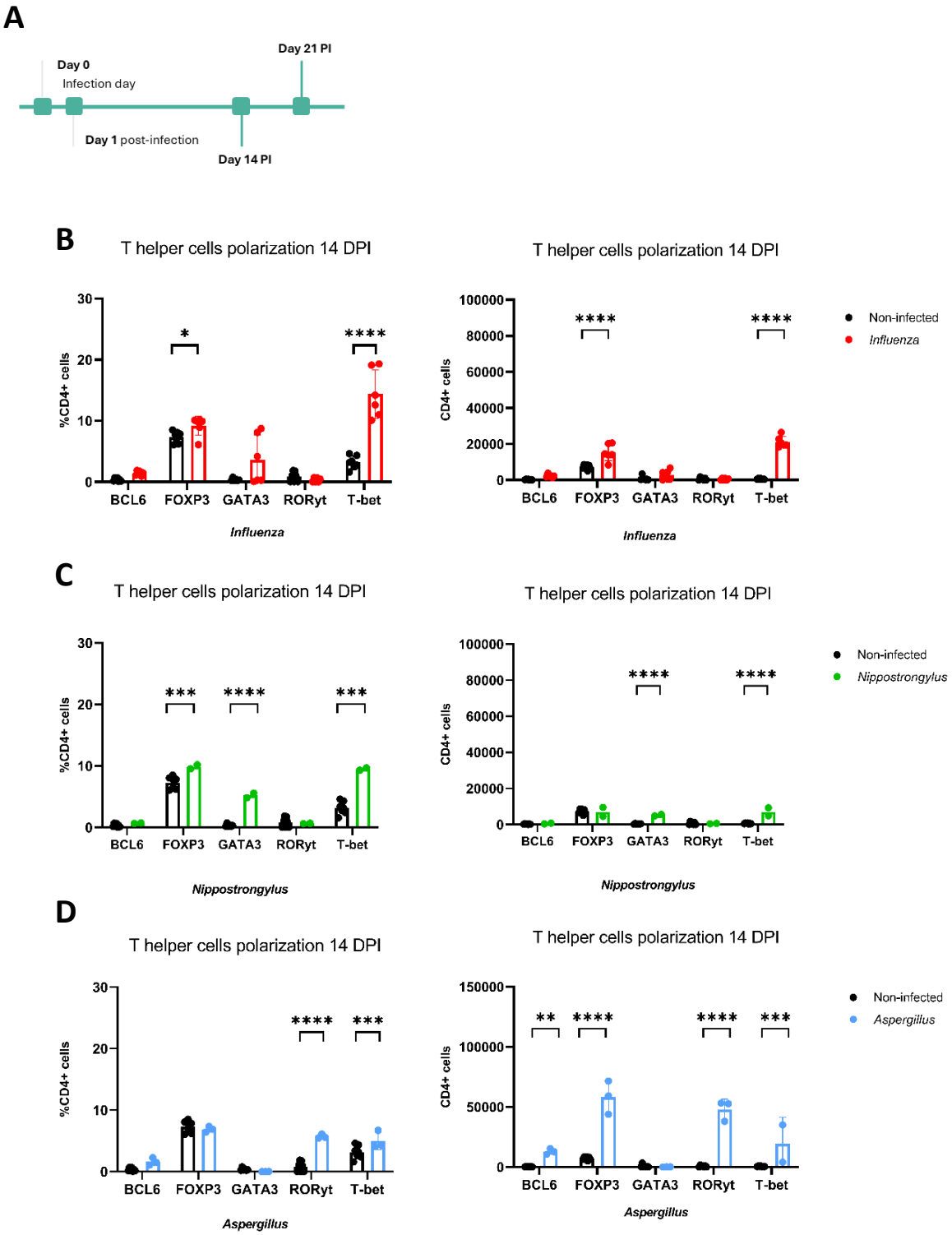

Figure 11- T helper cell polarization after infection (A) Experimental timeline showing 14 days post-infection for all infection models. **(B-D)** Bar plots illustrating the frequency (left) and absolute numbers (right) of intracellular marker expression in CD4+ T cells 14 days post-infection for **(B)** *Influenza*, **(C)** *Nippostrongylus*, and **(D)** *Aspergillus*. Statistical analysis was performed using two-way ANOVA followed by Sidak's multiple comparisons test to assess differences between non-infected and infected groups. Each dot represents a mouse.

Next, we examined *Nippostrongylus* infection **(Figure 11C),** where we expected a Th2 cell-dominant response due to the helminth nature of the infection. The results showed significant upregulation of GATA3, both in frequency **(Figure 11C, left)** and total cell numbers **(Figure 11C, right),** confirming the anticipated Type 2 polarization. However, we also observed an increase in T-bet expression, indicating that a Th1 cell response was also induced in *Nippostrongylus*-infected animals. Additionally, Foxp3 was elevated, suggesting that Tregs were activated as well. Despite the presence of both Th1 and Th2 cell pathways, the overall immune response was polarized towards Th2 cell, consistent with the type of pathogen, but with a notable Type 1 response. For *Aspergillus* infection **(Figure 11D),** we predicted a Th17 cell-dominant response, given that fungal infections typically elicit this type of immunity. The data confirmed this, with significant upregulation of RORγt, the Th17-associated transcription factor, in both frequency **(Figure 11D, left)** and total numbers **(Figure 11D, right).** Interestingly, we also observed upregulation of T-bet, indicating concurrent Th1 cell polarization. Furthermore, Bcl6, a marker for TFH cells, was notably expressed, suggesting that TFH cells were present in the lungs during *Aspergillus* infection, potentially contributing to a local immune response in the form of BALT. This finding supports the hypothesis that Th1 and Th17 cell immune responses can't be present independently, and in this case *Aspergillus* infection induces both Th1 and Th17 cell responses, while also engaging TFH cells to initiate local immune activity in the lungs. In conclusion, these results confirm our hypothesis that distinct T helper cell polarization occurs in response to different infections. *Influenza* infection predominantly induces a Th1 cell response, as evidenced by high T-bet expression, with additional Treg involvement. *Nippostrongylus* infection leads to Type 2 T cell responses, however both Th1 (T-bet) and Th2 (GATA3) cell pathways being activated, along with Treg expression. *Aspergillus* infection polarizes T cells into a type 3 response, marked by significant T-bet and RORγt expression, alongside TFH cell involvement in the lungs. These findings highlight the ability of different pathogens to drive specific immune polarization patterns, emphasizing the role of BALT as a local site for T cell priming and polarization.

4.6 BALT morphology on the lungs

The objective of this experiment was to visually confirm the formation of BALT in the lungs following infection with *Influenza*, *Nippostrongylus*, or *Aspergillus*. We aimed to determine whether BALT structures form in response to these infections and, if so, to characterize the

composition and organization of these structures, with the help of histology markers. If our hypothesis is correct, we expect to observe organized lymphoid structures containing both B and T cells, with BALT-like characteristics, particularly following infections that elicit a strong local immune response.

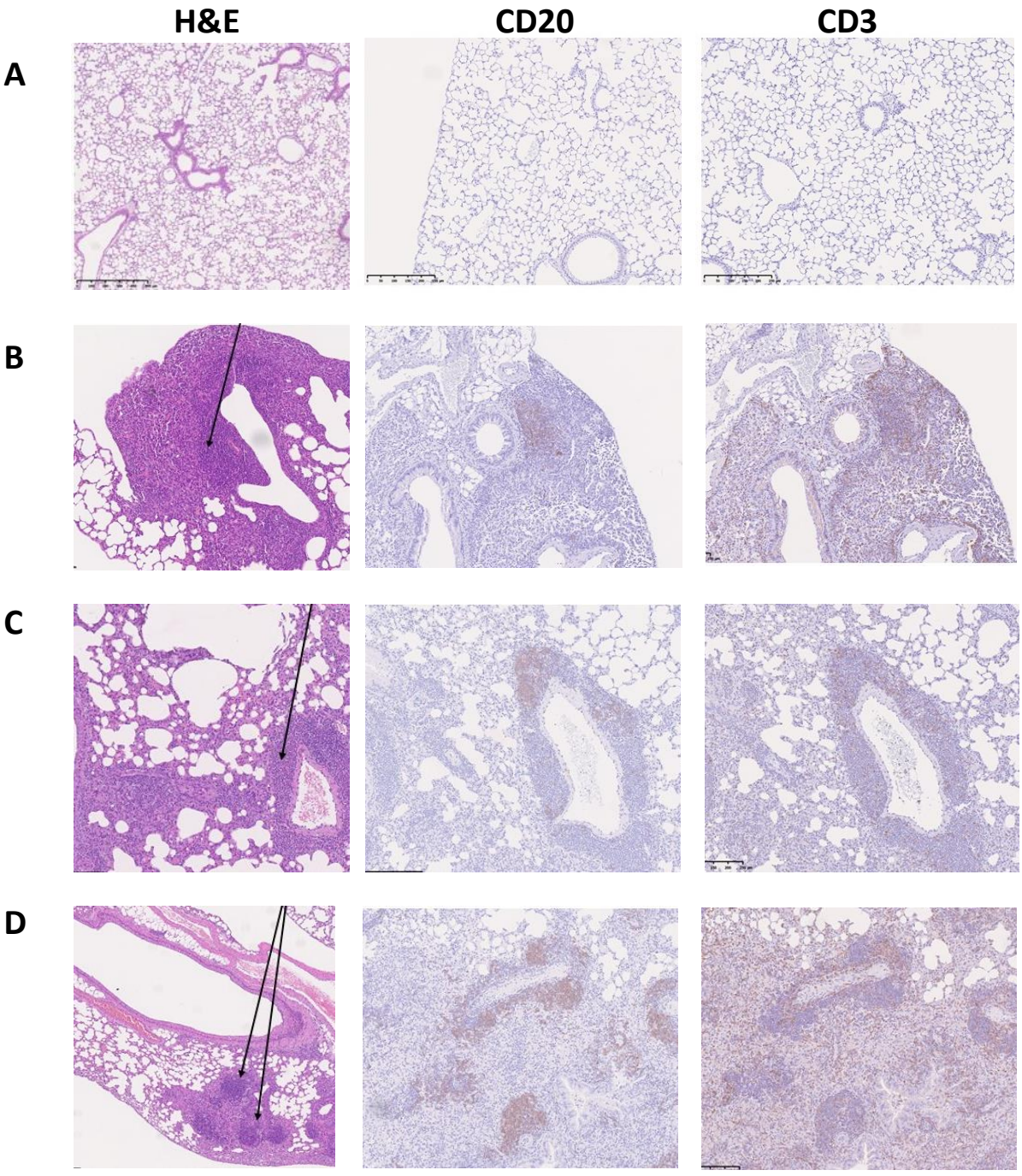

Figure 12- BALT is present in the lungs post-infection. (A-D) panel that shows histological analysis of lung tissues using H&E staining (left) and immune histochemistry staining for CD20 and CD3 (middle and right, respectively). **(A)** shows the lungs of non-infected control animals. **(B)** illustrates lungs from mice infected with *Influenza* **(C)** shows lungs from mice infected with *Nippostrongylus*. **(D)** histological cuts of lungs at 14 days post-*Aspergillus* infection. Each dot represents a mouse.

To test this, we analyzed lung tissue samples from infected mice at 14 days post-infection. Tissue morphology was examined using hematoxylin and eosin (H&E) staining, while immunohistochemistry (IHC) with CD3 (for T cells) and CD20 (for B cells) was chosen to identify the cellular composition of any potential lymphoid structures. The rationale of the experiment was to show the presence and formation of BALT in response to different infections. In non-infected animals **(Figure 12A),** histological analysis revealed normal lung morphology with no signs of immune cell infiltration or BALT formation. Both H&E staining **(Figure 12A, left)** and IHC for CD20 **(Figure 12A, middle)** and CD3 **(Figure 12A, right)** were negative, indicating the absence of significant lymphoid structures or clusters of immune cells.

In mice infected with *Influenza* **(Figure 12B),** we observed multifocal perivascular and peribronchiolar lymphoid infiltration in H&E-stained sections. However, these infiltrates lacked the organized follicular structures characteristic of mature BALT. IHC staining for CD3 and CD20 revealed dispersed T cells and small B cell clusters, suggesting an early immune response and the initiation of BALT formation. Similarly, in *Nippostrongylus*-infected mice **(Figure 12C),** we observed multifocal lymphoid infiltration in H&E-stained sections. However, as with the *Influenza* infection, there was no clear evidence of fully organized BALT. IHC staining showed small clusters of B cells with scattered T cells, indicating some immune cell activity and presumptive initial BALT formation. In contrast, *Aspergillus* infection resulted in more structured lymphoid organization. At 14 days post-infection **(Figure 12D)**, we observed significant lymphoid infiltration, with a follicle-like organization suggesting early BALT formation. By 21 days post-infection **(Figure S 7)**, we identified well-defined clusters of B cells and T cells in the lung tissue, strongly indicative of BALT-like structures. These more organized lymphoid clusters can be correlated with a more advanced state of BALT formation compared to the other infections.

Overall, these results support our hypothesis that BALT-like structures form in response to certain infections. Further staining should be performed in order to be able to make a more accurate diagnosis. While *Influenza* and *Nippostrongylus* infections induce some degree of lymphoid infiltration and immune cell clustering, indicative of early BALT formation, only *Aspergillus* infection led to the formation of more defined BALT structures. This suggests that BALT formation may be more strongly driven by certain types of infections, such as *Aspergillus*, which induce a more pronounced local immune response in the lungs.

Discussion

Understanding the triggers and mechanisms behind BALT formation is of great importance, as this knowledge could contribute to fill the gap regarding its role in respiratory diseases.

We hypothesized that BALT formation is induced in mice following infection with the recruitment of TFH cells. To test this hypothesis, we employed three distinct infection models: viral, fungal, and parasitic, each representing a different type of immune response. Testing different infection models enables us to examine BALT formation across diverse immune environments. In these models, we analyzed TFH cell recruitment and T cell polarization in lung post-infection, as well as BALT structure, using flow cytometry, histological analysis, and immunohistochemistry.

It is known that BALT can form in response to various infections, and its composition can vary based on the type of infections[21]. Nonetheless, the precise mechanisms and specific infections that consistently lead to the observation of BALT formation, the characterization of T cell polarization in the lung, and the confirmation of BALT formation through histopathological analysis of different infections, remain to be established.

While BALT formation following *Influenza* infection has been documented, its precise cellular composition and morphology are not fully characterized. In this study, we aimed to induce BALT via intranasal administration of *Influenza* X31, building on previous work from other groups that demonstrated BALT's role in respiratory immunity when dealing with this virus[22].

To assess BALT formation, we focused on two key cell populations in lung tissue: TFH cells and GC B cells. TFH cells were identified using PD-1 and CXCR5 markers, while GC B cells were characterized by GL-7 and CD95. These markers are well-established for identifying GCs in the spleen, and due to the similar cellular composition of BALT, we applied them to detect and analyze BALT formation in the lungs[40]. This allowed us to investigate the presence of these cells within BALT structures post-infection.

In our initial experiments, we did not detect CXCR5 expression in the lungs post-infection **(Figure 7D, F),** despite its clear presence in the spleen. To investigate this lack of CXCR5 expression, we processed the spleens, where a distinct TFH cell population had previously been observed **(Figure 7C, E),** using the same mechanical and enzymatic digestion techniques

applied to lung tissue. These results indicated that CXCR5 expression was masked during enzymatic digestion. Unlike tissues such as the spleen or LNs, which can often be dissociated mechanically, the lung's structure includes collagen and elastin, making it more resistant to mechanical dissociation. To overcome this, we used collagenase to break down collagen and DNase I to degrade DNA from dead cells during the digestion process, ensuring effective tissue dissociation[54].

It is important to note that enzymatic digestion can lead to the cleavage of surface receptors, including CXCR5 **(Figure 7D, F),** as seen in our work. To improve our protocol, we implemented two changes: we replaced the digestion enzyme with Liberase TL, and we extended the surface staining time from 15 minutes to 2 hours. The increase in the staining time allowed us to observe the re-expression of CXCR5, which had been cleaved during the enzymatic digestion[54] **(Figure S 4)**. Prior to addressing this issue with our protocol, we were able to characterize TFH-like cells that express several TFH cell markers, including PD-1 and ICOS. Usually this population is called TFH-like cells because it does not express CXCR5 and Bcl6. Our findings, that enzymatic digestion cleaves CXCR5, indicates that while CXCR5 is indeed present, it is often not detected in standard lung digestion protocols, which can lead to misleading results when analyzing this cell population. Many studies that attempt to characterize TFH cells in the lung have failed to identify a definitive TFH population, instead of labeling them as TFH-like. This discrepancy may arise from inadequate staining techniques[55] .

Besides these optimizations from the first experiments, we also infected animals with different viral loads. Although previous studies using similar viral doses had successfully demonstrated BALT formation[56], we opted to increase the dose of the *Influenza* virus to ensure a more robust immune response, since BALT usually is associated with chronic infection[20,21]. Following the optimization of the infection model, we chose a dose of 5000 PFU for intranasal administration, as this dosage resulted in elevated populations of TFH and TRM cells.

Our preliminary experiments identified the optimal time point for BALT formation following *Influenza* infection. It was used as a proxy to evaluate BALT formation the presence of TFH and GC B cells. This populations peaked at 14 days post-infection before gradually declining. These results align with previous reports indicating that day 14 is often the peak for lung-associated

immune populations[40]. In contrast, TFH cells in the mLNs, which drain the lungs, peaked around 21 days post-infection. This finding corroborates other studies indicating that immune cell populations associated with BALT maintain peak levels until later time points post-infection, in the dLNs[40]. High levels of TFH cells in these LNs, highlights the role of mLNs as primary draining nodes for the lungs, continuously filtering and presenting antigenic material.

To further analyze BALT formation following *Influenza* infection, we focused on day 14, which correspondes to the peak cell numbers in the previous experiment. The assessments were conducted by evaluating the lungs on day 14 and the mLNs on days 7, 14, and 21 post-infection. Our analysis revealed that the presence of TFH cells in the dLNs peaked on days 14 and 21 compared to non-infected controls. This is in line with our previous observations that TFH cell numbers were relatively low in the early post-infection time points but increased and persisted over time. In the lungs, 14 days post-infection, we analyzed TFH cells, GC B cells, and TRM cells, all of which were present following infection. We hypothesize that this is due to the formation of BALT.

Besides BALT formation following viral infections, other pathogens, have also been associated with BALT induction[21]. In this study, we aimed to determine whether BALT is formed following infections with *Aspergillus fumigatus*, a fungus, and *Nippostrongylus brasiliensis*, a helminth.

Previous studies have investigated *Aspergillus* infection as a potential trigger for BALT formation but concluded it was insufficient to induce BALT, with no follicular structures observed[57]. We predicted that their infection method may significantly contribute to these findings. The protocol used by these researchers involved a single infection with 10^7 conidia via oropharyngeal aspiration, which did not lead to BALT formation. In contrast, our approach has shown that intranasally infecting mice with 10^8 conidia in 30 µL and administering two doses, two days apart, led to a suboptimal infection[28]. Our results revealed the presence of BALT in the lungs 14 days post-infection, characterized by elevated frequencies of GC B cells, TFH cells, and TRM cells.

Similar observations were made in the mLNs, as the ones after *Influenza* infection, where the percentage of TFH cells was significantly higher compared to control groups, peaking in the dLNs at a later time point. Contributing to the previous knowledge that dLNs accumulate TFH

at later time points. This can be associated with dLNs being able to drain the lungs, once BALT is established.

In *Aspergillus* infection, the abundance of TRM cells in the lungs was significantly higher than in other infections. The increase of TRM cells in *Aspergillus* infected lungs **(Figure 10, E)** is in line with previous findings that report a high prevalence of CD8 TRM cells following *Aspergillus* exposure. The severity of this infection likely played a key role in eliciting a stronger immune response[28].

It has been previously shown and now confirmed the presence of BALT after type 1 and type 3 immune responses. However, its formation in the context of type 2 responses, such as those elicited by helminth infections, remains largely unexplored. We selected *Nippostrongylus brasiliensis*, to investigate whether BALT can also form following this infection, as it is commonly employed for eliciting robust Type 2 immune responses in the lung[28].

This infection is administered differently, using subcutaneous injections. Only two *N. Brasiliensis* infected lungs were analyzed. The results indicated low frequencies of GC B cells and TFH cells, but a high frequency of TRM cells. While these results are not conclusive, further experiments should be conducted to determine whether BALT is formed following *N. brasiliensis* infection. Notably, the high frequency of TRM cells observed in our study compared to non-infected controls suggests a robust local immune response, while previous studies have mentioned the existence of CD4 TRM cells after *N. brasiliensis* infection[58]. However, comparing the dLNs after *N. brasiliensis* infection, where TFH cells are present at early time points as well, with those following *Influenza* and *Aspergillus* infections, the tendency for TFH cells values to be higher at later time points post-infection changes. This is in agreement with our expectations, as the worms migrate from the lungs to the gut shortly after infection[59].

However, we still hypothesize that BALT can indeed form after *N. brasiliensis* infection, as other studies have demonstrated that this pathogen induces a Th2-type immune response and inflammation in the lungs[60].

In various immune responses, TFH cells can exhibit characteristics of other T helper cell subsets, reflecting their adaptability to different immunological contexts. To investigate T cell

polarization and its dependency on infection type, we analyzed CD4+ T helper cell polarization following three different infection models.

Influenza challenge elicited a strongly polarized Type 1 immune response, characterized by increased expression of T-bet. This result was expected since it has been seen before that *Influenza* infection usually does not polarize other T cell response[28]. Infection with *N. brasiliensis* also induced polarization towards a Type 2 immune response. However, T-bet levels were also upregulated compared to non-infected controls, this upregulation is consistent with existing results[28]. Analysis of T cell polarization following *Aspergillus* infection indicated a notable upregulation of RORγt, characteristic of Type 3 immune responses, alongside with high T-bet expression, when compared to control groups. This suggests a Type 3 immune response with increased frequency of Type 1 TF, corroborating findings from other studies that report similar patterns during *Aspergillus fumigatus* infection[28].

It is important to note that while one infection can elicit various immune responses, in our results we observed one predominant response that characterizes the immune reaction. Additionally, we observed the presence of Tregs after infection. This finding corroborates with existing literature, which indicates that once BALT forms, it recruits FoxP3+ Tregs to help modulate local inflammatory responses[21].

To visually confirm our results suggesting that BALT was formed, we aimed to assess tissue architecture and cellular organization using hematoxylin and eosin (H&E) staining and immunohistochemistry (IHC) **(Figure 12).** This approach allowed us to determine whether BALT is formed and how its characteristics vary with different types of infections. Histopathological assessments of infected lungs revealed notable differences in findings across these various infections.

In the case of *Influenza*, our results demonstrated evidence of BALT formation, characterized by perivascular and peribronchiolar lymphoid infiltration. We observed dispersed T cells intermingling among B cell clusters. These findings are consistent with early stages of BALT formation, where lymphoid structures begin to develop[33].

For *Nippostrongylus brasiliensis*, H&E staining revealed similar perivascular and peribronchiolar lymphoid infiltration. However, the absence of fully developed follicular

structures suggests that we observed only the initial stages of BALT formation, as in *Influenza*. Immunohistochemical analysis further confirmed the presence of small B cell clusters alongside dispersed T cells, which are characteristic of early BALT. Previous studies have also observed lymphocyte infiltration after *N. brasiliensis* infection that could be associated with BALT formation[60]. This preliminary lymphoid architecture suggests that the type 2 immune response elicited by helminth infections may stimulate the early development of BALT, although further experiments are required to validate and characterize these findings.

In the case of *Aspergillus*, for both time-points, we observed pronounced multifocal perivascular and peribronchiolar lymphoid infiltration, accompanied by follicle-like structures indicative of BALT. Notably, similar formations were documented in research in Pneumocystis-induced BALT formation[57]. Our immunohistochemical staining corroborated these observations, revealing distinct clusters of B and T cells.

However, it is essential to note that due to the limitations of our study, BALT formation remains presumptive. To confidently classify a pulmonary lymphoid cluster as BALT, it must exhibit a histologically observable B cell follicular structure, along with identifiable FDCs and T cells[61].

Further analyses of additional markers are necessary to accurately characterize these structures as BALT as well has higher number of analyzed samples.

Conclusion

This study provides new insights into the triggers for the formation of BALT. Our findings indicate that BALT formation is not solely induced by viral infections, such as Influenza, but also occurs in response to fungal and possibly parasitic pathogens, highlighting the capacity of this structure to form in response to stimuli. Notably, our results suggest that TFH cells are highly present in the lung after infection, which can be asscociated with the development of BALT. This highlights the lung's potential as a site for local T cell priming and demonstrates that TLS can form when appropriate stimuli are present. From being able to induce formation of this tissue, our findings offer valuable perspectives on how BALT can be leveraged to improve vaccination strategies, potentially enhancing respiratory infection control by manipulating local immune environments.

This will require addressing the limitations of the current study, such as the lack of IHC markers to accurately visualize BALT, the limited number of biological replicates, and the need to expand our spectral cytometry panel to characterize a broader range of cellular populations within this tissue, mainly to be able to observe TFH cells polarization in the lung. Additionally, ongoing experiments aim to investigate the lung microbiome following infection to assess its impact on BALT formation and to explore whether TFH cells generated by BALT correspond to specific subtypes based on their heterogeneity.

Supplementary Information

Table S1- Total number of mice used for each experiment per infection.

	C57BL/6J Mice			
Experiment	NI	IFZ	Nippo	Asp
Test IFZ infection	2	5	\	\
Different viral load	\	11	\	\
Different time points	\	11	\	\
BALT characterization	12	7	3	6
Histopathology	8	2	2	3
Microbiome Batch 1	6	21	21	21
Microbiome Batch 2	6	21	21	21
Total	34	78	47	51

Table S2- List of antibodies and concentrations used for flow cytometry (surface panel)

Specificity	Fluorophore	Clone	Company	Cat #	Dilution
CD4	eF506	RM4-5	Invitrogen	69-0042-82	1/400
CD8a	SB600	53-6.7	eBioscience	63-0081-82	1/400
TCRb	BV785	H57-597	Biolegend	109249	1/400
CD69	BV650	H1.2F3	Biolegend	104541	1/200
CD62L	APC	MEL-14	eBioscience	eBioscience	1/200
ICOS	PerCP/Cy5.5	C398.4A	Biolegend	313517	1/200
CD44	AF700	IM7	Biolegend	103026	1/400
CD279 (PD-1)	BV421	29F.IA12	Biolegend	135218	1/400
CD19	PacificB	6D5	Biolegend	115523	1/400
CD95 (Fas)	PE	Jo2	BD	554258	1/400
GL-7	AF647	GL-7	Biolegend	144606	1/200
L/D NIR				L10119	1/6000

Table S3- List of antibodies and concentrations used for flow cytometry (Intracellular panel)

Specificity	Fluorophore	Clone	Company	Cat #	Titration
FoxP3	eF450	FJK-16s	eBioscience	48-5773-82	1/400
T-bet	PE-Cy7	4B10	BL	644824	1/400
RoRg(t)	APC	B2D	eBioscience	17-6988-80	1/400
GATA3	PE	TWAJ	Invitrogen	12-9966-42	1/400
CD4	eF506	RM4-5	Invitrogen	69-0042-82	1/400
CD8a	SB600	53-6.7	eBioscience	63-0081-82	1/400
TCRb	BV785	H57-597	BL	109249	1/400
Bcl6	AF647	K112-91	BD	561525	1/400
L/D NIR				L10119	1/6000

Table S4- Histology antibodies for immunohistochemistry (IHC)

Specificity	Clone	Company	Cat #	Dilution
CD20	SP32	Abcam	ab64088	1:75
CD3	Polyclonal	Agilent	IR50361-2	RTU

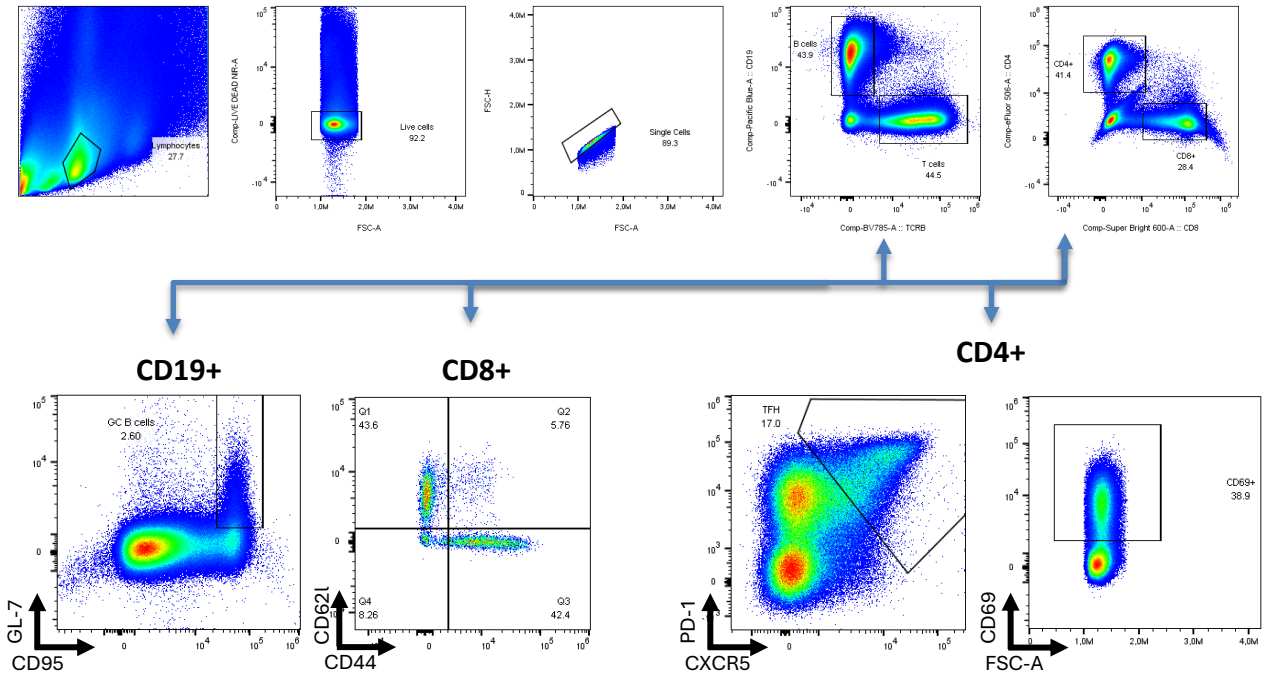

Figure S 1- Gating Strategy. The gating strategy used to analyse all cells isolated from C57BL/6 mice is described for spleen cell populations, including lymphocytes, live cells, single cells, T and B cells, and CD4+ and CD8+ T cells. First, lymphocytes were gated based on side scatter (SSC-A) vs. forward scatter (FSC-A) characteristics to isolate the lymphocyte population. In the second step, singlet cells were identified by gating FSC-H vs. FSC-A to exclude doublets. The third step involved distinguishing live and dead cells using the LiveDead marker (NIR), which stains dead cells with compromised membranes, producing intense fluorescence due to the dye's reaction with free amines. In the fourth step, B and T cells were differentiated by staining CD19 (PacBlue) for B cells and TCRβ (BV785) for T cells. Within the TCRβ+ population, CD8+ and CD4+ T cells were further distinguished. Now using the analysis of the lungs its described how we further separate cell populations. For CD8+ T cells, additional gating with CD62L (APC) and CD44 (AF700) identified effector cells. CD4+ T cells were analysed for TFH (CD4+ CXCR5+ PD-1+) using ef506, PE-Cy7, and PE fluorochromes. Additionally, within the CD4+ population, TRM cells were identified by gating on CD69 and FSC-A in lung tissue analysis. For B cell analysis, GC B cells were identified within the CD19+ population using GL-7 and CD95 markers.

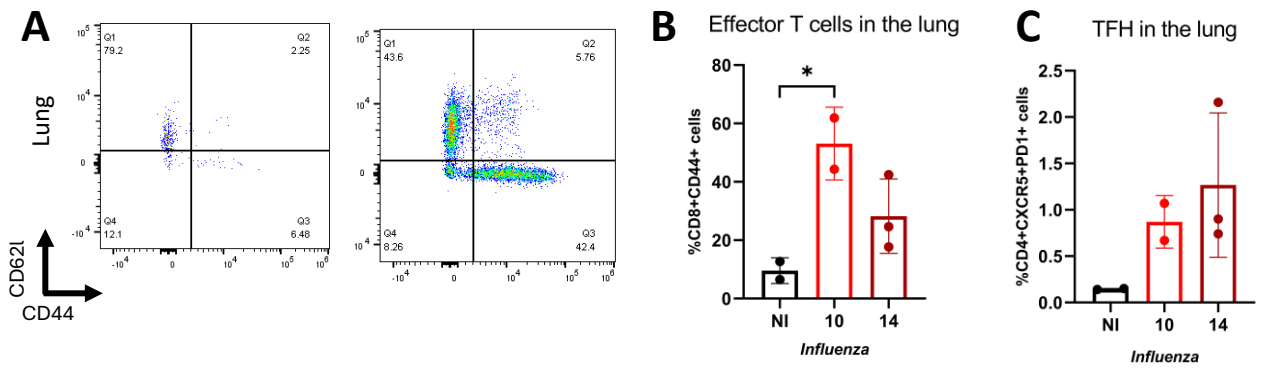

Figure S 2- Surface Staining Shows CXCR5 cleavage in the Lungs During Digestion (A) Dot plots and **(B)** Histogram showing the recruitment of effector CD8+ T cells after infection in the lung. **(C)** Histogram showing absolute numbers of TFH cells in the lungs. Each dot represents a mouse.

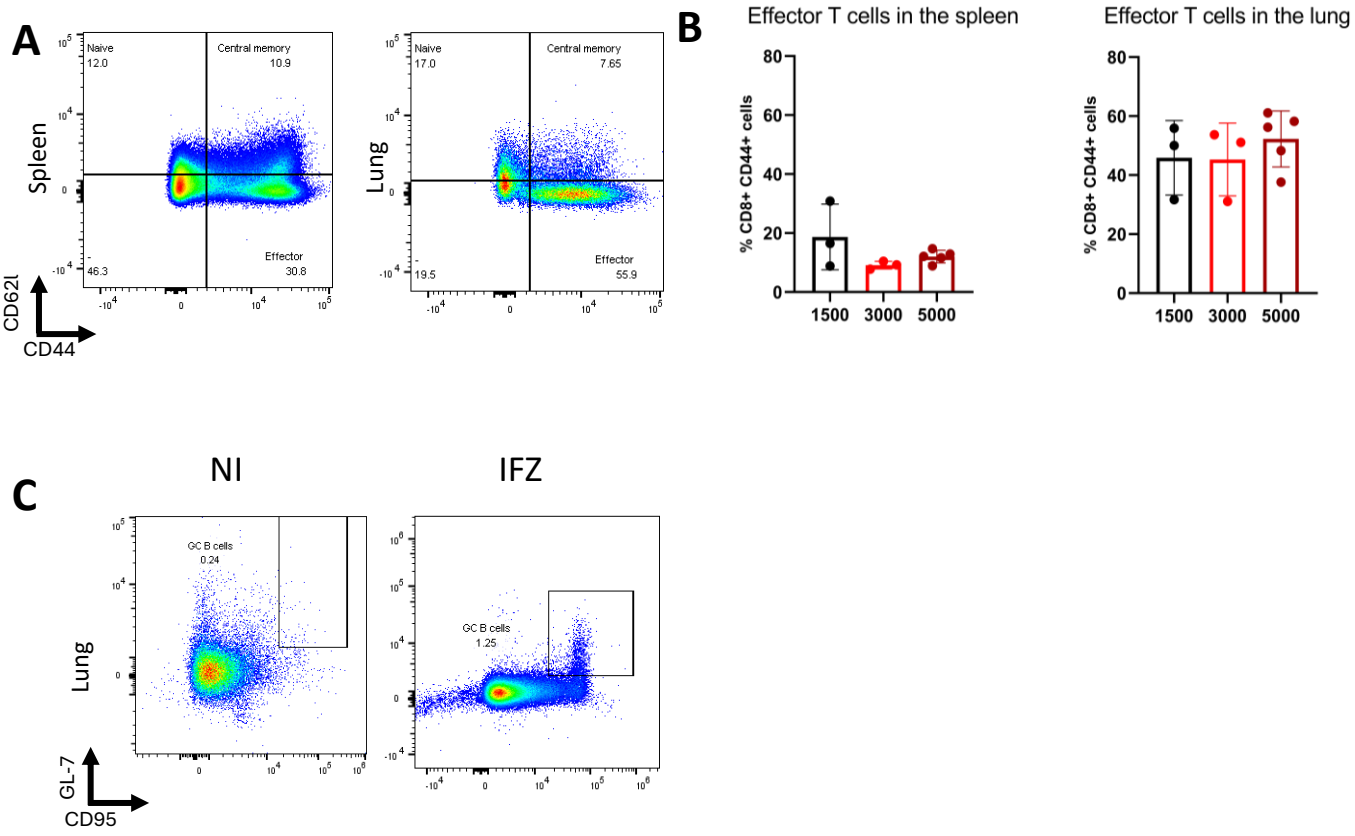

Figure S 3- Optimal *Influenza* Viral Load for Inducing BALT Formation. (A) Dot plots and **(B)** Histogram showing the recruitment of effector CD8+ T cells after infection in the spleen (left) and lung (right). Each dot represents a mouse.

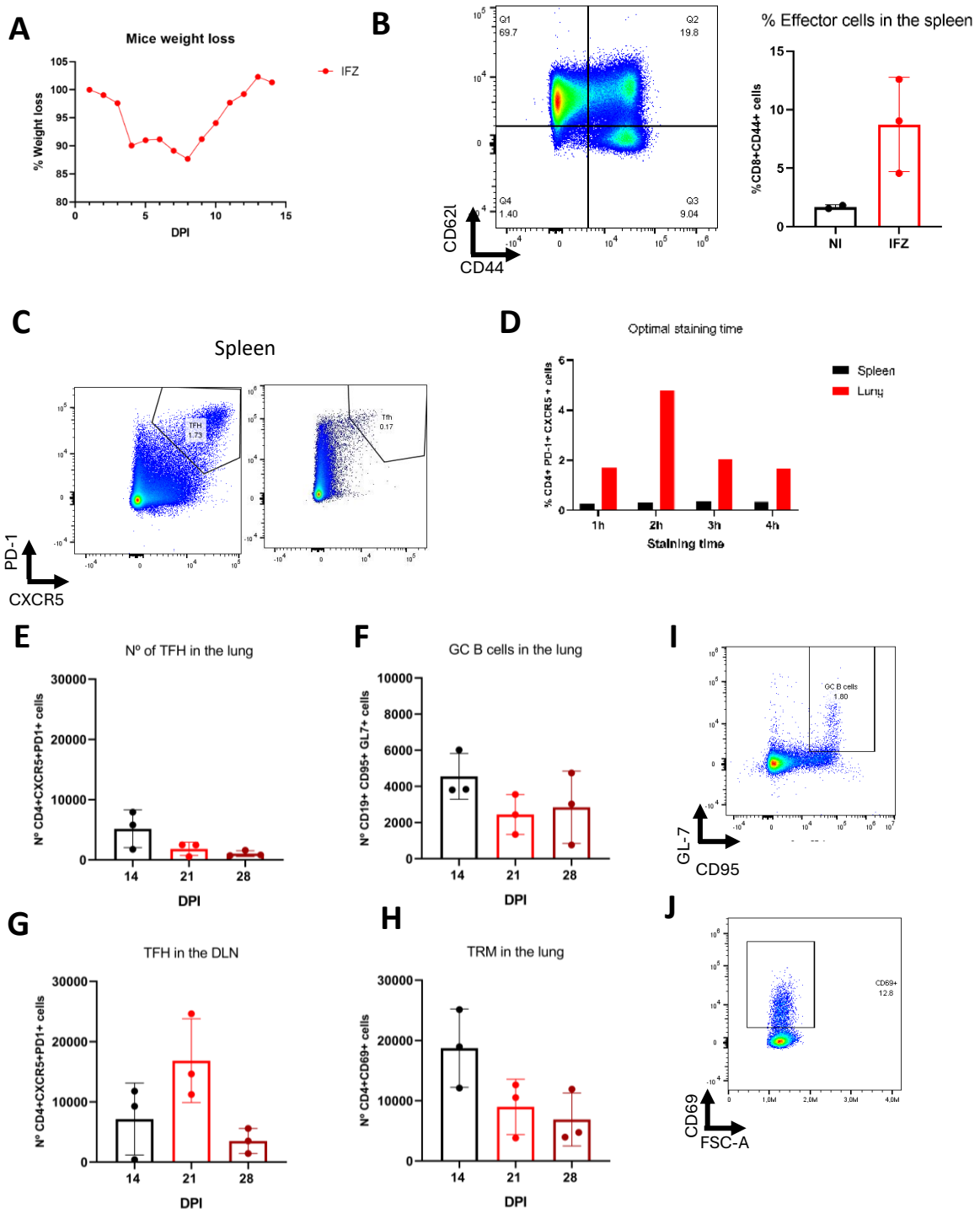

Figure S 4 BALT Formation and Immune Cell Dynamics at Different Time Points Following *Influenza* Infection (A) Mice weight loss. **(B)** Dot plots and histogram showing recruitment of effector CD8+ T cells after infection. **(C)** CXCR5 expression in the spleen without (left) and after enzymatic digestion (right) . **(D)** Optimal staining time, showing CXCR5 expression with different timestamps for surface staining in both lung and spleen tissue. **(E-H)** Total cell numbers of **(E)** TFH cells in the draining lung, **(F)** GC B cells in the lung, **(G)** TFH cells in the dLNs, and **(H)** TRM cells in the lung. **(I-J)** Representative dot plots showing **(I)** GC B cells in the lung, and **(J)** TRM cells. Each dot represents a mouse.

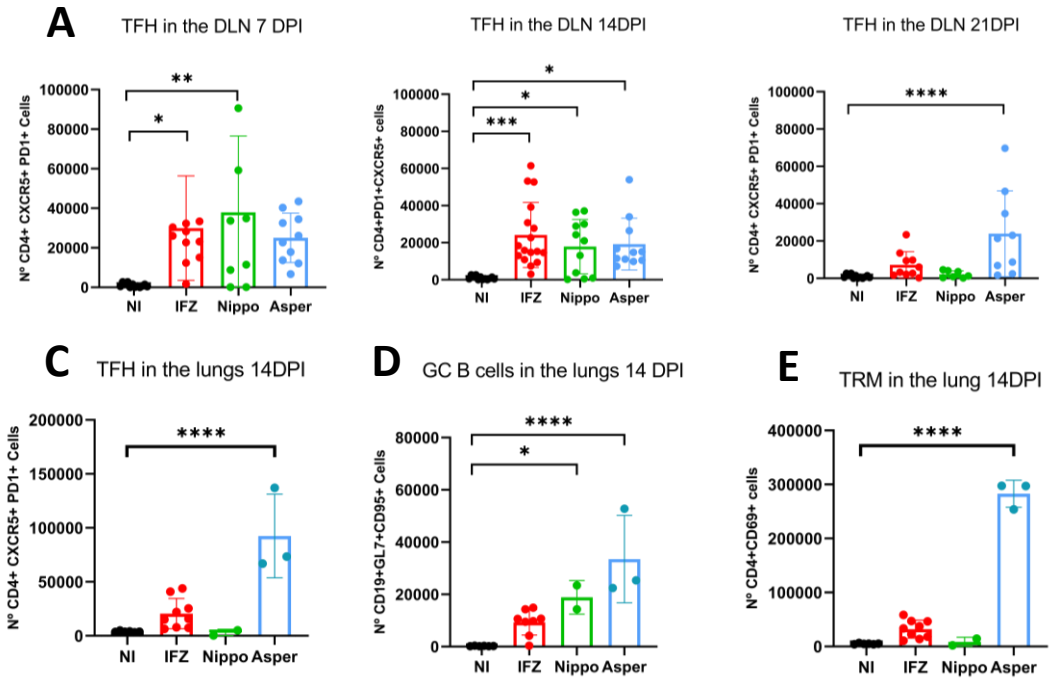

Figure S 5 BALT is formed upon three different infection types (A) Dot plots displaying the immune cell populations present in the lungs after infection. **(B-E)** Histogram plots representing the absolute cell numbers of various immune cell populations at different time points post-infection. **(B)** Absolute numbers of T follicular helper (TFH) cells in the draining LN at 7 days (left), 14 days (middle), and 21 days (right) post-infection. **(C)** Absolute numbers of TFH cells in the lungs 14 days post-infection. **(D)** GC (germinal center) B cells in the lungs at 14 days post-infection. **(E)** TRMT cells (TRM) in the lungs at 14 days post-infection. Each dot represents a mouse.

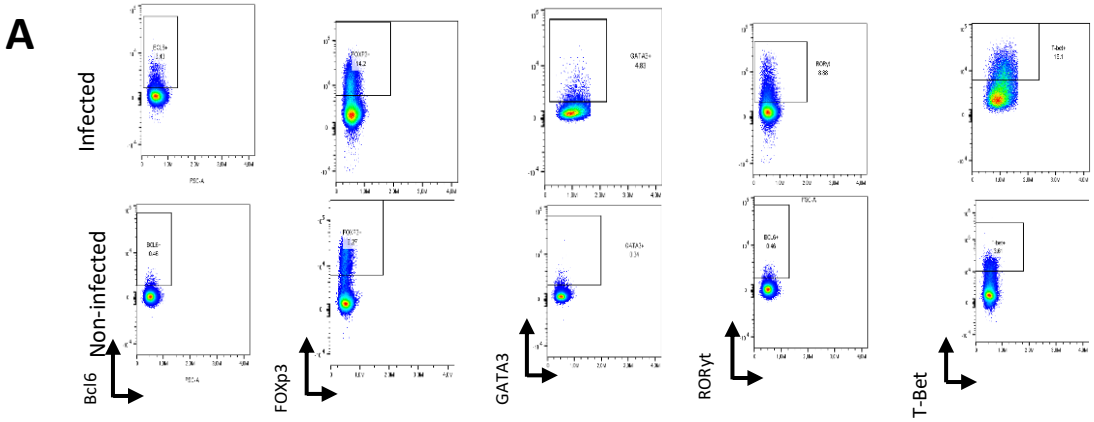

Figure S 6 T helper cell polarization in the lung. (A-E) Dot plots showing the polarization of T helper cell subsets in non-infected versus infected animals. **(A)** Bcl6 expression, **(B)** FOXP3 expression, **(C)** GATA3 expression, **(D)** RORγt expression, and **(E)** T-bet expression. Each dot represents a mouse.

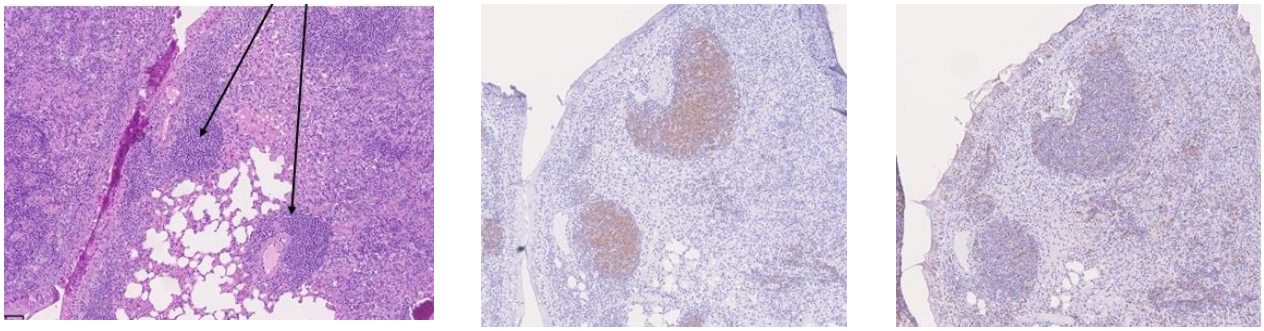

Figure S 7- BALT morphology. (A) BALT is present in the lungs 21 days post *Aspergillus* infection showing three different staining's H&E (left), CD20 (middle) for B cells and CD3 (right) for T cells

References

1. Saleh A, Qamar S, Tekin A, Singh R, Kashyap R. Vaccine Development Throughout History. *Cureus*. 13(7):e16635. doi: 10.7759/cureus.16635

2. Gilbert SC. T-cell-inducing vaccines – what's the future. *Immunology*. 2012;135(1):19-26. doi: 10.1111/j.1365-2567.2011.03517.x

3. Chaplin DD. Overview of the Immune Response. *J Allergy Clin Immunol*. 2010;125(2 Suppl 2):S3-23. doi: 10.1016/j.jaci.2009.12.980

4. Sun L, Su Y, Jiao A, Wang X, Zhang B. T cells in health and disease. *Signal Transduct Target Ther*. 2023;8(1):235. doi: 10.1038/s41392-023-01471-y

5. Victora GD, Nussenzweig MC. Germinal Centers. *Annu Rev Immunol*. 2022;40:413-442. doi: 10.1146/annurev-immunol-120419-022408

6. Yu D, Walker LSK, Liu Z, Linterman MA, Li Z. Targeting TFH cells in human diseases and vaccination: rationale and practice. *Nat Immunol*. 2022;23(8):1157-1168. doi: 10.1038/s41590-022-01253-8

7. Kim S, Shah SB, Graney PL, Singh A, Singh A. Multiscale engineering of immune cells and lymphoid organs. *Nat Rev Mater*. 2019;4(6):355-378. doi: 10.1038/s41578-019-0100-9

8. Murphy K. *Janeway's Immunobiology*. 9th edition. Garland Science/Taylor & Francis Group, LLC; 2017.

9. Randall TD, Carragher DM, Rangel-Moreno J. Development of secondary lymphoid organs. *Annu Rev Immunol*. 2008;26:627-650. doi: 10.1146/annurev.immunol.26.021607.090257

10. Randall TD, Mebius RE. The development and function of mucosal lymphoid tissues: a balancing act with micro-organisms. *Mucosal Immunol*. 2014;7(3):455-466. doi: 10.1038/mi.2014.11

11. Stebegg M, Kumar SD, Silva-Cayetano A, Fonseca VR, Linterman MA, Graca L. Regulation of the Germinal Center Response. *Front Immunol*. 2018;9. doi: 10.3389/fimmu.2018.02469

12. Gitlin AD, Mayer CT, Oliveira TY, et al. T cell help controls the speed of the cell cycle in germinal center B cells. *Science*. 2015;349(6248):643-646. doi: 10.1126/science.aac4919

13. Anang DC, Balzaretti G, van Kampen A, de Vries N, Klarenbeek PL. The Germinal Center Milieu in Rheumatoid Arthritis: The Immunological Drummer or Dancer? *Int J Mol Sci*. 2021;22(19):10514. doi: 10.3390/ijms221910514

14. Batista FD, Harwood NE. The who, how and where of antigen presentation to B cells. *Nat Rev Immunol*. 2009;9(1):15-27. doi: 10.1038/nri2454

15. Corsiero E, Nerviani A, Bombardieri M, Pitzalis C. Ectopic Lymphoid Structures: Powerhouse of Autoimmunity. *Front Immunol*. 2016;7. doi: 10.3389/fimmu.2016.00430

16. Vinuesa CG, Linterman MA, Yu D, MacLennan ICM. Follicular Helper T Cells. *Annu Rev Immunol*. 2016;34:335-368. doi: 10.1146/annurev-immunol-041015-055605

17. Crotty S. Follicular helper CD4 T cells (TFH). *Annu Rev Immunol*. 2011;29:621-663. doi: 10.1146/annurev-immunol-031210-101400

18. Schumacher TN, Thommen DS. Tertiary lymphoid structures in cancer. *Science*. 2022;375(6576):eabf9419. doi: 10.1126/science.abf9419

19. Shinoda K, Hirahara K, Iinuma T, et al. Thy1+IL-7+ lymphatic endothelial cells in iBALT provide a survival niche for memory T-helper cells in allergic airway inflammation. *Proc Natl Acad Sci U S A*. 2016;113(20):E2842-2851. doi: 10.1073/pnas.1512600113

20. Manzo A, Bombardieri M, Humby F, Pitzalis C. Secondary and ectopic lymphoid tissue responses in rheumatoid arthritis: from inflammation to autoimmunity and tissue damage/remodeling. *Immunol Rev*. 2010;233(1):267-285. doi: 10.1111/j.0105-2896.2009.00861.x

21. Silva-Sanchez A, Randall TD. Role of iBALT in respiratory immunity. *Curr Top Microbiol Immunol*. 2020;426:21-43. doi: 10.1007/82_2019_191

22. Moyron-Quiroz JE, Rangel-Moreno J, Kusser K, et al. Role of inducible bronchus associated lymphoid tissue (iBALT) in respiratory immunity. *Nat Med*. 2004;10(9):927-934. doi: 10.1038/nm1091

23. Ribeiro F, Perucha E, Graca L. T follicular cells: The regulators of germinal center homeostasis. *Immunol Lett*. 2022;244:1-11. doi: 10.1016/j.imlet.2022.02.008

24. Song W, Craft J. T Follicular Helper Cell Heterogeneity. *Annu Rev Immunol*. 2024;42(1):127-152. doi: 10.1146/annurev-immunol-090222-102834

25. Overacre-Delgoffe AE, Bumgarner HJ, Cillo AR, et al. Microbiota-specific T follicular helper cells drive tertiary lymphoid structures and anti-tumor immunity against colorectal cancer. *Immunity*. 2021;54(12):2812-2824.e4. doi: 10.1016/j.immuni.2021.11.003

26. Kaufmann SHE, Kabelitz D. 1 - The Immune Response to Infectious Agents. In: Kabelitz D, Kaufmann SHE, eds. *Methods in Microbiology*. Vol 37. Immunology of Infection. Academic Press; 2010:1-20. doi: 10.1016/S0580-9517(10)37001-2

27. Kumar S, Basto AP, Ribeiro F, et al. Specialized Tfh cell subsets driving type-1 and type-2 humoral responses in lymphoid tissue. *Cell Discov*. 2024;10(1):1-21. doi: 10.1038/s41421-024-00681-0

28. Barros L, Piontkivska D, Figueiredo-Campos P, et al. CD8+ tissue-resident memory T-cell development depends on infection-matching regulatory T-cell types. *Nat Commun*. 2023;14(1):5579. doi: 10.1038/s41467-023-41364-w

29. Szabo PA, Miron M, Farber DL. Location, location, location: Tissue resident memory T cells in mice and humans. *Sci Immunol*. 2019;4(34):eaas9673. doi: 10.1126/sciimmunol.aas9673

30. Turner DL, Bickham KL, Thome JJT, et al. Lung Niches for the Generation and Maintenance of Tissue-resident Memory T cells. *Mucosal Immunol*. 2014;7(3):501-510. doi: 10.1038/mi.2013.67

31. Bienenstock J, McDermott MR. Bronchus- and nasal-associated lymphoid tissues. *Immunol Rev*. 2005;206(1):22-31. doi: 10.1111/j.0105-2896.2005.00299.x

32. Bienenstock J, Johnston N, Perey DY. Bronchial lymphoid tissue. I. Morphologic characteristics. *Lab Investig J Tech Methods Pathol*. 1973;28(6):686-692.

33. Randall TD. Bronchus-associated lymphoid tissue (BALT) structure and function. *Adv Immunol*. 2010;107:187-241. doi: 10.1016/B978-0-12-381300-8.00007-1

34. Sautès-Fridman C, Petitprez F, Calderaro J, Fridman WH. Tertiary lymphoid structures in the era of cancer immunotherapy. *Nat Rev Cancer*. 2019;19(6):307-325. doi: 10.1038/s41568-019-0144-6

35. Pitzalis C, Jones GW, Bombardieri M, Jones SA. Ectopic lymphoid-like structures in infection, cancer and autoimmunity. *Nat Rev Immunol*. 2014;14(7):447-462. doi: 10.1038/nri3700

36. Hwang JY, Silva-Sanchez A, Carragher DM, Garcia-Hernandez M de la L, Rangel-Moreno J, Randall TD. Inducible Bronchus-Associated Lymphoid Tissue (iBALT) Attenuates Pulmonary Pathology in a Mouse Model of Allergic Airway Disease. *Front Immunol*. 2020;11:570661. doi: 10.3389/fimmu.2020.570661

37. Matsumoto R, Gray J, Rybkina K, et al. Induction of bronchus-associated lymphoid tissue is an early life adaptation for promoting human B cell immunity. *Nat Immunol*. 2023;24(8):1370-1381. doi: 10.1038/s41590-023-01557-3

38. Dieu-Nosjean MC, Antoine M, Danel C, et al. Long-Term Survival for Patients With Non–Small-Cell Lung Cancer With Intratumoral Lymphoid Structures. *J Clin Oncol*. 2008;26(27):4410-4417. doi: 10.1200/JCO.2007.15.0284

39. Koroleva EP, Fu YX, Tumanov AV. Lymphotoxin in physiology of lymphoid tissues - implication for antiviral defense. *Cytokine*. 2018;101:39-47. doi: 10.1016/j.cyto.2016.08.018

40. Tan HX, Esterbauer R, Vanderven HA, Juno JA, Kent SJ, Wheatley AK. Inducible Bronchus-Associated Lymphoid Tissues (iBALT) Serve as Sites of B Cell Selection and Maturation Following Influenza Infection in Mice. *Front Immunol*. 2019;10:611. doi: 10.3389/fimmu.2019.00611

41. Allman D, Jain A, Dent A, et al. BCL-6 Expression During B-Cell Activation. *Blood*. 1996;87(12):5257-5268. doi: 10.1182/blood.V87.12.5257.bloodjournal87125257

42. Tunyaplin C, Shaffer AL, Angelin-Duclos CD, Yu X, Staudt LM, Calame KL. Direct repression of prdm1 by Bcl-6 inhibits plasmacytic differentiation. *J Immunol Baltim Md 1950*. 2004;173(2):1158-1165. doi: 10.4049/jimmunol.173.2.1158

43. Crotty S. A brief history of T cell help to B cells. *Nat Rev Immunol*. 2015;15(3):185-189. doi: 10.1038/nri3803

44. Förster R, Mattis AE, Kremmer E, Wolf E, Brem G, Lipp M. A Putative Chemokine Receptor, BLR1, Directs B Cell Migration to Defined Lymphoid Organs and Specific Anatomic Compartments of the Spleen. *Cell*. 1996;87(6):1037-1047. doi: 10.1016/S0092-8674(00)81798-5

45. Gunn MD, Ngo VN, Ansel KM, Ekland EH, Cyster JG, Williams LT. A B-cell-homing chemokine made in lymphoid follicles activates Burkitt's lymphoma receptor-1. *Nature*. 1998;391(6669):799-803. doi: 10.1038/35876

46. Johnston RJ, Poholek AC, DiToro D, et al. Bcl6 and Blimp-1 are reciprocal and antagonistic regulators of T follicular helper cell differentiation. *Science*. 2009;325(5943):1006-1010. doi: 10.1126/science.1175870

47. Choi YS, Yang JA, Yusuf I, et al. Bcl6 expressing follicular helper CD4 T cells are fate committed early and have the capacity to form memory. *J Immunol Baltim Md 1950*. 2013;190(8):4014-4026. doi: 10.4049/jimmunol.1202963

48. Baumjohann D, Okada T, Ansel KM. Cutting Edge: Distinct waves of BCL6 expression during T follicular helper cell development. *J Immunol Baltim Md 1950*. 2011;187(5):2089-2092. doi: 10.4049/jimmunol.1101393

49. Reif K, Ekland EH, Ohl L, et al. Balanced responsiveness to chemoattractants from adjacent zones determines B-cell position. *Nature*. 2002;416(6876):94-99. doi: 10.1038/416094a

50. Yusuf I, Kageyama R, Monticelli L, et al. Germinal center T follicular helper cell IL-4 production is dependent on signaling lymphocytic activation molecule receptor (CD150). *J Immunol Baltim Md 1950*. 2010;185(1):190-202. doi: 10.4049/jimmunol.0903505

51. Ettinger R, Sims GP, Fairhurst AM, et al. IL-21 induces differentiation of human naive and memory B cells into antibody-secreting plasma cells. *J Immunol Baltim Md 1950*. 2005;175(12):7867-7879. doi: 10.4049/jimmunol.175.12.7867

52. Qi H, Cannons JL, Klauschen F, Schwartzberg PL, Germain RN. SAP-controlled T-B cell interactions underlie germinal centre formation. *Nature*. 2008;455(7214):764-769. doi: 10.1038/nature07345

53. Shi J, Hou S, Fang Q, Liu X, Liu X, Qi H. PD-1 Controls Follicular T Helper Cell Positioning and Function. *Immunity*. 2018;49(2):264-274.e4. doi: 10.1016/j.immuni.2018.06.012

54. Couillault C, Germain C, Dubois B, Kaplon H. Identification of Tertiary Lymphoid Structure-Associated Follicular Helper T Cells in Human Tumors and Tissues. In: Dieu-Nosjean MC, ed. *Tertiary Lymphoid Structures: Methods and Protocols*. Springer; 2018:205-222. doi: 10.1007/978-1-4939-8709-2_12

55. Vu Van D, Beier KC, Pietzke LJ, et al. Local T/B cooperation in inflamed tissues is supported by T follicular helper-like cells. *Nat Commun*. 2016;7(1):10875. doi: 10.1038/ncomms10875

56. Boyden AW, Legge KL, Waldschmidt TJ. Pulmonary infection with influenza A virus induces site-specific germinal center and T follicular helper cell responses. *PloS One*. 2012;7(7):e40733. doi: 10.1371/journal.pone.0040733

57. Eddens T, Elsegeiny W, Garcia-Hernadez M de la L, et al. *Pneumocystis*-Driven Inducible Bronchus-Associated Lymphoid Tissue Formation Requires Th2 and Th17 Immunity. *Cell Rep*. 2017;18(13):3078-3090. doi: 10.1016/j.celrep.2017.03.016

58. Thawer SG, Horsnell WG, Darby M, et al. Lung-resident CD4+ T cells are sufficient for IL-4Rα-dependent recall immunity to Nippostrongylus brasiliensis infection. *Mucosal Immunol*. 2014;7(2):239-248. doi: 10.1038/mi.2013.40

59. Silveira MR, Nunes KP, Cara DC, et al. Infection with Strongyloides venezuelensis Induces Transient Airway Eosinophilic Inflammation, an Increase in Immunoglobulin E, and Hyperresponsiveness in Rats. *Infect Immun*. 2002;70(11):6263-6272. doi: 10.1128/IAI.70.11.6263-6272.2002

60. Harvie M, Camberis M, Tang SC, Delahunt B, Paul W, Le Gros G. The Lung Is an Important Site for Priming CD4 T-Cell-Mediated Protective Immunity against Gastrointestinal Helminth Parasites. *Infect Immun*. 2010;78(9):3753-3762. doi: 10.1128/IAI.00502-09

61. Pabst R. Plasticity and heterogeneity of lymphoid organs. What are the criteria to call a lymphoid organ primary, secondary or tertiary? *Immunol Lett*. 2007;112(1):1-8. doi: 10.1016/j.imlet.2007.06.009